INTERNATIONAL CENTER FOR AGGREGATES RESEARCH

ICAR

FIELD VALIDATION OF THE CROSS-ANISOTROPIC BEHAVIOR OF UNBOUND AGGREGATE BASES

RESEARCH REPORT ICAR - 502-2

Sponsored by the
Aggregates Foundation
for Technology, Research and Education

Technical Report Documentation Page

1. Report No. ICAR/502-2	2. Government Accession No.	3. Recipient's Catalog No.
4. Title and Subtitle FIELD VALIDATION OF THE CROSS-ANISOTROPIC BEHAVIOR OF UNBOUND AGGREGATE BASES		5. Report Date July 2001 6. Performing Organization Code
7. Author(s) Erol Tutumluer, Alex Adu-Osei, Dallas N. Little, and Robert L. Lytton		8. Performing Organization Report No. Report No. 502-2
9. Performing Organization Name and Address Texas Transportation Institute The Texas A&M University System College Station, Texas 77843-3135		10. Work Unit No. (TRAIS) 11. Contract or Grant No. Project No. 404001
12. Sponsoring Agency Name and Address Aggregates Foundation for Technology, Research, and Education 2101 Wilson Blvd, Suite 100 Arlington, VA 22201-3062		13. Type of Report and Period Covered March 2001 14. Sponsoring Agency Code

15. Supplementary Notes
Research performed in cooperation with International Center for Aggregates Research and Aggregates Foundation for Technology, Research, and Education.
Research Project Title: Structural Characteristics of Unbound Aggregate Bases to Meet AASHTO Design Requirements

16. Abstract

The ICAR Research Project 502 has focused on determining structural considerations of unbound aggregate pavement layers for a proper representation in the new AASHTO Pavement Design Guide 2002. The research team developed models for the resilient and permanent deformation behavior from the results of triaxial tests conducted at the Texas Transportation Institute (TTI) and at the University of Illinois. The studies have mainly indicated that the unbound aggregate base (UAB) material should be modeled as nonlinear and cross-anisotropic to account for stress sensitivity and the significant differences between vertical and horizontal moduli and Poisson's ratios.

UABs were constructed at the TTI Riverside research facility and tested for response and performance using the one-third scale model of the Texas Mobile Loading Simulator. The resilient responses of the test sections were modeled. The nonlinear cross-anisotropic material models used in the base layer predicted vertical deflections that are close to field deflections in the analyzed TTI pavements.

Field validation data were also collected from a full-scale pavement test study conducted at Georgia Tech. The test sections had extensive instrumentation and the pavement response variables, such as stresses, strains, and deformations, were measured in all pavement layers including the UABs. The validation of the anisotropic modeling approach was accomplished by analyzing these test sections using GT-PAVE finite element program, predicting UAB responses, and comparing them to the measured ones. Laboratory testing of the aggregate samples was conducted at the University of Illinois and the characterization models were developed for the stress sensitive, cross-anisotropic aggregate behavior. With nonlinear anisotropic modeling of the UAB, the resilient behavior of pavement test sections was successfully predicted at the same time for a number of response variables. In addition, the stress sensitive, cross-anisotropic representation of the base was shown to greatly reduce the horizontal tension computed in the granular base when compared to a linear isotropic representation.

17. Key Words unbound aggregate base cross-anisotropic unbound granular materials	18. Distribution Statement No restrictions. This document is available to the public through NTIS: National Technical Information Service 5285 Port Royal Road Springfield, Virginia 22161		
19. Security Classif.(of this report) Unclassified	20. Security Classif.(of this page) Unclassified	21. No. of Page 80	22. Price

Form DOT F 1700.7 (8-72) **Reproduction of completed page authorized**

FIELD VALIDATION OF THE CROSS-ANISOTROPIC BEHAVIOR OF UNBOUND AGGREGATE BASES

by

Erol Tutumluer
Assistant Professer
University of Illinois at Urbana-Champaign

Alex Adu-Osei
Graduate Research Assistant
Texas A&M University

Dallas N. Little
Senior Research Fellow
Texas A&M University

and

Robert L. Lytton
Research Engineer
Texas Transportation Institute
Texas A&M University

Report No 502-2

Project No. 404001
Research Report Title: Structural Characteristics of Unbound Aggregate Bases to Meet AASHTO Design Requirements

Sponsored by
Aggregates Foundation for Technology, Research and Education

March 2001

Texas A&M University
TEXAS TRANSPORTATION INSTITUTE
College Station, Texas 77840
MS 3135

DISCLAIMER

The contents of this report reflect the views of the authors, who are responsible for the facts and the accuracy of the data presented herein. The contents do not necessarily reflect the official views or policies of the International Center for Aggregate Research (ICAR), Texas Transportation Institute (TTI), or Texas A&M University. The report does not constitute a standard, specification, or regulation, nor is it intended for construction, bidding, or permit purposes.

TABLE OF CONTENTS

PAGE

Introduction 1

Summary of ICAR Research Efforts in Structural Characterization of UABs 2

Report Organization 5

TTI Test Sections 7

Data Analysis 12

Georgia Tech Test Sections 16

GT-PAVE Finite Element Program 17

Nonlinear Solution Technique 18

Georgia Tech Full-Scale Pavement Test Study 21

Test Section Construction 25

Performance of the Test Sections 25

Laboratory Evaluation of Norcross Crushed Stone at the University of Illinois 26

Description and Capabilities of the UI-FastCell 28

Material Properties 29

Resilient Modulus Testing 32

Modeling of Georgia Tech Pavement Test Sections 35

Material Properties Assigned in the Early Work by Tutumluer (1995) 36

Test Section Resilient Response Predictions by Tutumluer (1995) 39

Test Section Response Predictions from Linear Elastic Analyses 41

Test Section Response Predictions from Nonlinear Isotropic Analyses 44

Test Section Response Predictions from Nonlinear Anisotropic Analyses 47

A Simlified Procedure for Determining Anisotropic Model Parameters 48

Stress States from Anisotropic Modeling 57

TABLE OF CONTENTS

Page

Summary and Conculsions 60

TTI Pavement Test Sections 60

Georgia Tech Pavement Test Sections 61

Research Needs for Implementation 65

References 67

LIST OF TABLES

Table Page

1. Falling Weight Deflectometer Data on TTI Pavement Section 12 9
2. Multi-Depth Deflectometer Data on TTI Pavement Section 12 10
3. Falling Weight Deflectometer Data on TTI Pavement Section 11 10
4. Multi-Depth Deflectometer Data on TTI Pavement Section 11 11
5. Backcalculated Material Properties for TTI Pavement Section 12..... 14
6. Backcalculated Material Properties for TTI Pavement Section 11..... 14
7. Average Percent Errors of Deflections for TTI Pavement Section 12..... 15
8. Average Percent Errors of Deflections for TTI Pavement Section 11..... 15
9. Geometry and Performance Summary of Georgia Tech Pavement Test Sections (after Barksdale and Todres, 1983) 23
10. Aggregate Gradations and Material Properties Used in Flexible Pavement Test Sections 24
11. Detailed Summary of Resilient Test Section Response..... 27
12. Modified Proctor (AASHTO T-180) Properties of Georgia Tech Base Course Aggregates 30
13. Achieved Dry Densities and Moisture Contents for All Modulus Test Samples 32
14. Model Parameters for Vertical Moduli: ICAR Protocol and AASHTO T294-94 Tests..... 34
15. Material Properties and Model Parameters Used in Modeling Pavement Test Section Response (after Tutumluer, 1995) 38
16. Comparison of Predicted and Measured Response Variables (after Tutumluer, 1995) 40
17. Linear Elastic Base Properties Used in Modeling Pavement Test Section Response 41
18. Comparison of Predicted and Measured Response Variables for Conventional Pavement Sections – Linear Elastic Analyses 42
19. Comparison of Predicted and Measured Response Variables for Inverted Pavement Sections – Linear Elastic Analyses 43
20. Isotropic Model Parameters Used in Modeling Pavement Test Section Response 44

LIST OF TABLES (con't)

Table Page

21. Comparison of Predicted and Measured Response Variables for Conventional Pavement Sections – Nonlinear Isotropic 45
22. Comparison of Predicted and Measured Response Variables for Inverted Pavement Sections – Nonlinear Isotropic 46
23. Anisotropic Model Parameters Used in Modeling Pavement Test Section Response..... 47
24. Comparison of Predicted and Measured Response Variables for Conventional Pavement Sections – Nonlinear Anisotropic 52
25. Comparison of Predicted and Measured Response Variables for Inverted Pavement Sections – Nonlinear Anisotropic 53

LIST OF FIGURES

Figure Page

1. The Multi-Depth Deflectometer Sensor 8
2. TTI Pavement Sections with MDD Sensor Locations 8
3. Measured Surface and Depth Deflections on TTI Pavement Section 12 11
4 .Measured Surface and Depth Deflections on TTI Pavement Section 11 12
5. Resilient Modulus Search Technique Using Secant Stiffnesses for the Stress Hardening Granular Material Behavior 20
6. The University of Illinois FastCell (UI-FastCell) Triaxial Testing Device 29
7. Gradation Curves for Norcross Crushed Stone and Other Georgia Tech Base Materials 31
8. Variation of Vertical Moduli with Deviator Stresses from AASHTO T294-94 Tests 34
9. K-θ Models Showing Variation of Vertical Moduli with Bulk Stresses 35
10. Typical Cross Sections of Georgia Tech Pavement Test Sections 36
11. Variation of Constant Ratios in Horizontal and Shear Stiffness Ratio Models (after Tutumluer and Thompson, 1998) 49
12. Variation of Stress Exponents in the Horizontal Stiffness Ratio Model (after Tutumluer and Thompson, 1998) 50
13. Variation of Stress Exponents in the Shear Stiffness Ratio Model (after Tutumluer and Thompson, 1998) 50
14. Vertical Modulus Distribution within the Base Predicted by Texas-3 Model 55
15. Modular Ratio (M_R^h/M_R^v) Distribution within the Base Predicted by Texas-3 Model 56
16. Vertical Modulus Distribution within the Base Predicted by AASHTO T294-94 Model 57
17. Distribution of Centerline Radial Stresses within the Base Predicted by Different Analyses 58

INTRODUCTION

As of 2000, over 4 billion tons of aggregates, crushed stone, sand, and gravel, are produced annually in the United States. A large quantity of this material goes into the construction of pavements. In flexible pavements, and especially for thinly surfaced pavements, the unbound granular layers serve as major structural components of the pavement system. Methods that more realistically characterize unbound aggregate bases (UABs) could significantly improve the ability to reliably predict unstabilized pavement response, which in turn would lead to better design methodology. With increasing demands being placed on highways through heavier and increasing number of loads it is critical that we be able to better characterize the unbound aggregates component of the highway by incorporating recent advances in our characterization such as the anisotropic, stress dependent behavior.

Existing and past pavement design procedures have generally taken a very conservative view of the relative strength properties of unbound granular materials. There has been a recent move towards the use of mechanistic-empirical approaches to design and analyze pavement structures. The National Cooperative Highway Research Program (NCHRP) has funded the development of the new AASHTO Pavement Design Guide – 2002. This guide will establish the structural contribution of various materials used as pavement layers including the unbound aggregate bases and subbases. It is essential that the structural contribution assigned to aggregate layers in this new guide and in its subsequent versions is as accurate as possible since this structural characterization will be used for pavement design and analysis well into the 21st century. Therefore, it is of utmost importance for the aggregate industry to make available laboratory test data, field performance data, and other information to support the most accurate structural characterization possible of unbound aggregate used in the pavement structure.

In order for aggregate to be economically more competitive, and also to expand the existing markets for utilization of more aggregate, as realized by industry, there is an imminent need to provide continuing support for the ongoing research efforts at the International Center for Aggregates Research (ICAR). These efforts have been primarily aimed at enhancing the understanding of the actual anisotropic, stress dependent behavior of UABs and better

characterization of the excellent compressive characteristics of the high quality aggregates for proper representation in the newly developed AASHTO 2002 Design Guide and its future versions.

SUMMARY OF ICAR RESEARCH EFFORTS IN STRUCTURAL CHARACTERIZATION OF UABS

The ICAR Research Project 502 has focused on determining structural considerations of unbound aggregate pavement layers for a proper representation in the new *AASHTO Pavement Design Guide – 2002*. The research team has developed models for the resilient and permanent deformation behavior from the results of triaxial tests conducted at the Texas Transportation Institute (TTI) and at the University of Illinois. The models account for the stress dependent behavior at selected low, intermediate, and high stress states and explain the anisotropic properties of the UABs. The studies have mainly indicated that the unbound aggregate base material should be modeled as nonlinear and cross-anisotropic to account for stress sensitivity and the significant differences between vertical and horizontal moduli and Poisson's ratios.

- The research team also developed a testing protocol that, while significantly different from the AASHTO T294-94 protocol, is not more complicated. The protocol uses three stress regimes and ten stress levels within each regime to determine stress sensitivity and cross anisotropy. A laboratory test matrix was developed to study the resilient and permanent deformation behavior of four granular materials. The effects of moisture, gradation, compaction method, and material type on the deformational response of granular materials were also studied. Using as inputs the measured material response (strains) from tests, a Systems Identification (SID) approach has been developed to determine five material properties necessary to properly characterize the aggregate base and to satisfy the requirements of elastic work potential theory. These five material properties, needed to define a cross-anisotropic material under conditions of axial symmetry, are:
    - resilient moduli in vertical and radial directions,
    - M_R^z and M_R^r; shear modulus in vertical direction,
    - G_R; Poisson's ratio for strain in the vertical direction due to a horizontal direct stress, and

- ν_z; and Poisson's ratio for strain in any horizontal direction due to a horizontal direct stress, ν_r.

The new material models and testing protocol represent a significantly improved method for analyzing the structural performance of unbound aggregates in pavement layers. A Uzan type model, which relates the resilient modulus to both bulk and deviator stresses, has been found to properly characterize the stress dependency of granular materials.

Uzan (1985) Model: $$M_R = K_A\left(\frac{\theta}{P_0}\right)^{K_B}\left(\frac{\sigma_d}{P_0}\right)^{K_C} \quad (1)$$

where $\theta = \sigma_1 + \sigma_2 + \sigma_3$ = bulk stress,

$\sigma_d = \sigma_1 - \sigma_3$ = deviator stress,

P_0 = unit reference pressure (1 psi or 1 kPa), and

K_A, K_B, K_C = material constants obtained from repeated load triaxial tests.

The three cross-anisotropic moduli, each modeled by the same stress-dependent Uzan type functional form (Uzan, 1985), have, therefore, the following model parameters:

		θ	σ_d
	Coefficient	Exponent	Exponent
1. *Horizontal Resilient Modulus*, M_R^H:	K_1 = constant (psi),	K_2,	K_3
2. *Vertical Resilient Modulus*, M_R^V:	K_4 = constant (psi),	K_5,	K_6
3. *Resilient Shear Modulus*, G_R:	K_7 = constant (psi),	K_8,	K_9

where K_1 to K_9 obtained from SID scheme replace for each modulus the model parameters K_A, K_B, and K_C. Note that this report uses the vertical and horizontal moduli (M_R^H and M_R^V) interchangeably with the modulus in z-direction, M_R^z, and the modulus in r-direction, M_R^r, and the shear modulus is given either as G or G_R.

Alternatively, anisotropic modular ratios m and n can also be expressed in the same stress dependent form as:

	Coefficient	θ Exponent	σ_d Exponent
• $n = M_R^H / M_R^V$:	K_1 / K_4 = constant,	K_2-K_5,	K_3-K_6
• $m = M_R^H / G_R$	K_7 / K_4 = constant,	K_8-K_5,	K_9-K_6

Development of these advanced aggregate characterization models is an ongoing research effort to provide the essential input data into the finite element programs for adequately predicting the behavior and field stress states. The existing GT-PAVE and TTI-PAVE finite element (FE) programs have been modified to accommodate the developed anisotropic nonlinear material characterization models for the analysis of the UABs. A new post-processor/graphical visualization software package has been adopted for use with the GT-PAVE program. In addition, for improving FE inputs and ease in the modeling efforts, an MS Visual Basic™ user interface has been developed for the GT-PAVE program.

The ICAR 502 project has considered several methods of UAB characterization for comparison and field validation. These include:

(1) a linear elastic, isotropic analysis,
(2) a linear elastic, cross-anisotropic analysis,
(3) a nonlinear, stress sensitive isotropic analysis,
(4) characterization of the vertical resilient modulus as nonlinear stress sensitive according to a Uzan type model and then assuming that the horizontal modulus is some percentage of the vertical modulus (Tutumluer, 1995),
(5) a nonlinear stress sensitive cross-anisotropic analysis using modulus models developed following the laboratory SID approach (Adu-Osei et al., 2000), and
(6) a nonlinear stress sensitive cross-anisotropic analysis with model parameters obtained from a simplified procedure that uses AASHTO T294-94 resilient modulus test results and adopted earlier by Tutumluer and Thompson (1998).

REPORT ORGANIZATION

The previous ICAR 502 project reports documented the development of a methodology to characterize the cross-anisotropic nature of unbound aggregate base materials and to explain the difference such a characterization makes in terms of stress distribution within the aggregate base. It was indicated that the stress distribution is more realistic than that developed when the aggregate base is considered to be linear and isotropic. The stress distribution based on cross-anisotropic analysis is not only more correct, but it is also more favorable to the unbound aggregate in that significant tensile stresses do not occur. This report documents the validation of the various UAB characterization methods by analyzing pavement test sections using TTI-PAVE and GT-PAVE FE programs, by predicting UAB responses, and by comparing them to the measured ones.

Field validation data were collected from two previous full-scale pavement test studies. The first study deals with two flexible pavement test sections built at the Texas Transportation Institute (TTI) Research Annex. The first pavement had a thin asphalt surface layer while the second one had a thick asphalt surface layer. The base course in each pavement was a crushed Texas limestone meeting Texas Department of Transportation (TxDOT) Grade 1, Item 248, aggregate base specifications. These test sections were instrumented with multi-depth deflectometers (MDDs). A falling weight deflectometer (FWD) was positioned directly over the MDD and at several different positions away from MDD and pavement response (deflections) were collected. Analyses used FWD data to backcalculate material properties of the two pavement sections. For validation of the anisotropic resilient behavior, the limestone was characterized in the laboratory according to the ICAR testing protocol and pavement deflections were computed using the TTI-PAVE FE program. The predicted deflections are compared in this report to the measured deflections in the field. Of particular interest will be the comparison of accuracy of deflection predictions among linear isotropic, nonlinear isotropic, and nonlinear cross-anisotropic systems.

Another full-scale pavement test study, which had extensive instrumentation done and the responses measured in the UABs, was conducted by Barksdale and Todres, (1983) A Study of Factors Affecting Crushed Stone Base Performance. The pavements studied with granular bases

consisted of 3 conventional sections and two inverted sections with cement stabilized subbases. An inverted section is constructed by placing in a flexible pavement an unbound aggregate base sandwiched between an upper asphalt concrete surfacing and a lower cement stabilized subbase. Each test measured a total of eight response parameters, stresses and strains at different locations in the test sections together with surface deflections.

The aggregate material used in the granular base layers of the Georgia Tech pavement test sections was a granitic gneiss, referred to in this report as the Norcross crushed stone, which was obtained from the Norcross Quarry of Vulcan Materials Co. Laboratory testing of the aggregate samples was conducted at the University of Illinois and the characterization models were developed for the stress sensitive, cross-anisotropic aggregate behavior. The resilient responses of the Georgia Tech full-scale test sections were then predicted using the GT-PAVE FE program for a complete suite of different characterization and pavement analysis methods discussed earlier. The predictions made in the current study are compared to the measured responses in this most comprehensive finite element modeling effort to validate the cross-anisotropic characterization of UABs undertaken in the ICAR 502 project.

TTI TEST SECTIONS

The cross-anisotropic resilient model developed from the ICAR test protocol and the SID approach was verified with field data collected on two pavement sections at the TTI Research Annex. The data used in the field validation were originally collected in a study conducted by Uzan and Scullion (1990) to verify backcalculation procedures. The pavement sections were instrumented with multi-depth deflectometers (MDD). Falling weight deflectometer loads were applied to the pavement surfaces and pavement response (deflections) were collected. Pavement deflections were determined using the TTI-PAVE finite element program and compared to deflections measured in the field. The effect of using different material models to characterize unbound granular layers on deflections was also studied.

The multi-depth deflectometer measures the resilient deflection and permanent deformation in pavement layers. Figure 1 shows a schematic diagram of the MDD sensor. The MDD consists of modules with LVDTs positioned at different depths in the pavement to measure vertical movement in the layers. A maximum of six MDD sensors may be located in a single hole. The field installation and calibration are described elsewhere (Scullion et al., 1988).

The two pavement sections had different layer thicknesses. Section 11 had a thin surfacing over a thick crushed limestone base over a sandy gravel subgrade. Section 12 had a thick surface layer over a thick crushed limestone base over a sandy gravel subgrade. The MDD anchors are located at 1.625 and 2.025 meters in the thin and thick sections, respectively. The thin pavement had two MDD sensors and the thick pavement had four. Figure 2 shows the pavement layer thicknesses and MDD sensor locations.

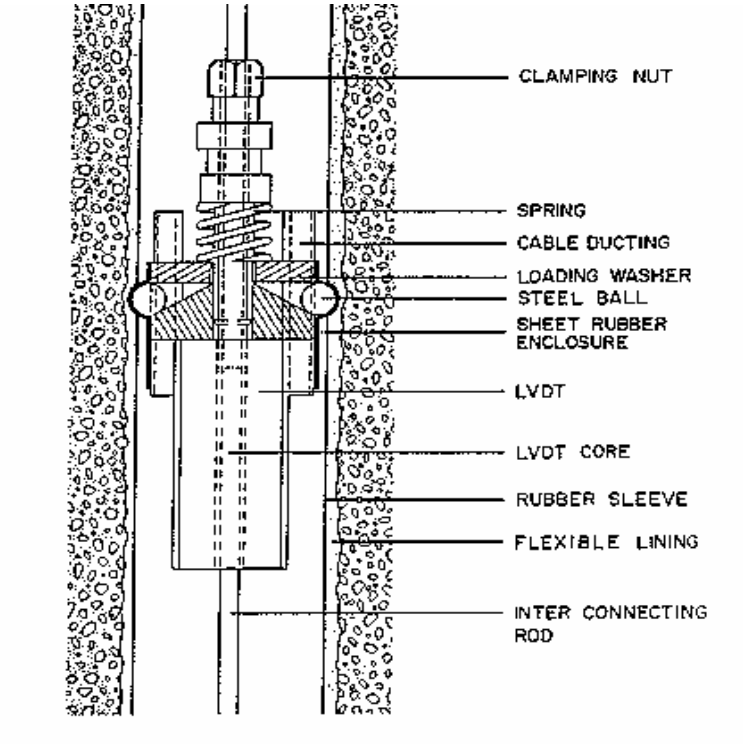

Figure 1. The Multi-Depth Deflectometer Sensor

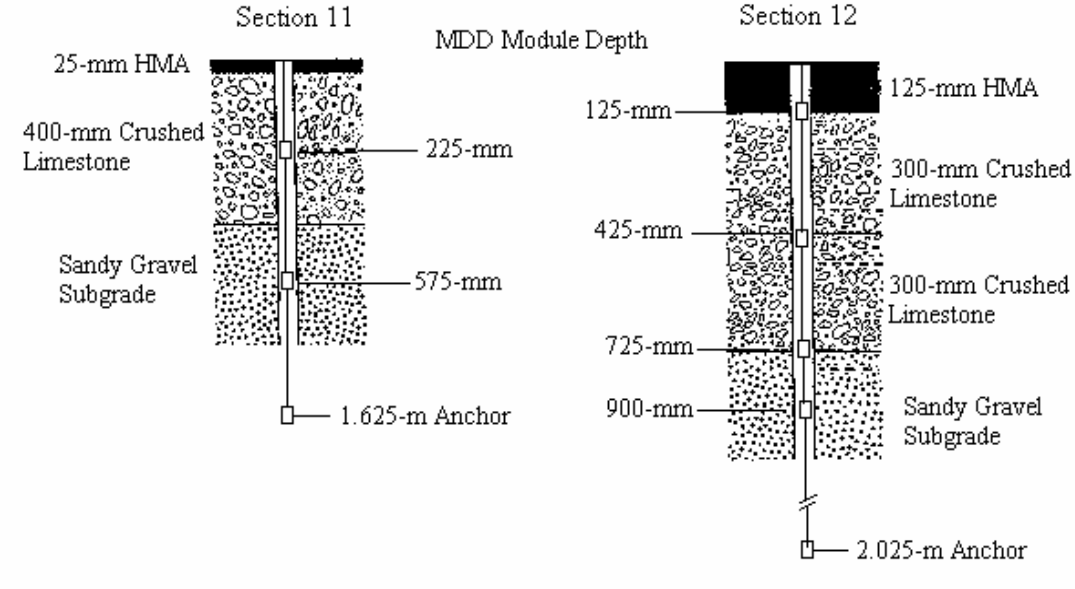

Figure 2. TTI Pavement Sections with MDD Sensor Locations

The FWD load plate was placed close to the MDD hole and four different load levels (approximately 28.9, 40.0, 46.7 and 64.5-kN) were applied. Data collectors recorded surface deflections (FWD sensors), depth deflections (MDD sensors) and MDD anchor movement. The MDD anchor movement was measured with a FWD sensor placed on the MDD setup. Replicate readings were taken at each load level.

The FWD load plate was then repositioned at several distances from the MDD hole and the test repeated. Thus, two-dimensional deflection bowls were recorded using this technique.

The average FWD results for the thick pavement (section 12) are shown in Table 1 and the corresponding MMD depth deflections (40.0-kN level only) and anchor movements are shown in Table 2. The values in parentheses are normalized deflections, in deflection per unit load. Similar results for the thin pavement (section 11) are shown in Tables 3 and 4. The FWD and MDD data are plotted in Figures 3 and 4 for sections 12 and 11, respectively.

Table 1. Falling Weight Deflectometer Data on TTI Pavement Section 12

Load	FWD Surface Deflections, in μm and (μm/kN)					
(kN)	Radial Distance (m)					
	0.0	0.3	0.6	0.9	1.2	1.8
28.9	140.7 (4.9)	91.9 (3.2)	52.8 (1.8)	36.6 (1.3)	27.7 (1.0)	16.8 (0.6)
40.0	196.1 (4.9)	131.1 (3.3)	77.7 (1.9)	52.1 (1.3)	40.4 (1.0)	25.9 (0.6)
46.7	234.7 (5.0)	159.5 (3.4)	94.7 (2.0)	64.5 (1.4)	48.3 (1.0)	33.5 (0.7)
64.5	323.6 (5.0)	216.7 (3.4)	131.1 (2.0)	90.4 (1.4)	67.1 (1.0)	47.0 (0.7)

Table 2. Multi-Depth Deflectometer Data on TTI Pavement Section 12

Load (kN)	Distance from Load to MDD (m)	Deflection at Depth (μm) MDD Location (m)				Anchor
		0.125	0.425	0.725	0.900	2.025
40.0	0.2	152.1	114.8	92.5	78.0	37.6
40.0	0.4	116.3	98.0	84.3	72.9	37.1
40.0	0.5	95.0	84.1	75.9	67.1	35.3
40.0	0.7	61.7	60.2	60.7	55.9	32.8
40.0	1.1	43.7	45.0	47.8	45.5	30.5

Table 3. Falling Weight Deflectometer Data on TTI Pavement Section 11

Load (kN)	FWD Surface Deflection, in μm and (μm/kN) Radial Distance (m)					
	0.0	0.3	0.6	0.9	1.2	1.8
28.9	324.6 (11.2)	125.2 (4.3)	57.4 (2.0)	38.1 (1.3)	30.5 (1.1)	26.2 (0.9)
42.8	449.8 (10.5)	193.8 (4.5)	87.4 (2.0)	59.2 (1.4)	47.8 (1.1)	40.6 (0.9)
64.5	632.2 (9.8)	289.6 (4.4)	132.1 (2.0)	90.4 (1.4)	73.7 (1.1)	62.2 (1.0)

Table 4. Multi-Depth Deflectometer Data on TTI Pavement Section 11

Load (kN)	Distance from Load to MDD (m)	Deflection at Depth (μm) MDD Location (m)		Anchor
		0.225	0.575	1.625
42.8	0.23	295.4	185.9	67.6
42.8	0.48	150.1	142.5	68.3
42.8	0.78	76.2	79.0	51.3
64.5	0.23	428.8	299.5	106.9
64.5	0.48	215.9	206.5	99.6
64.5	0.78	117.3	123.7	82.3

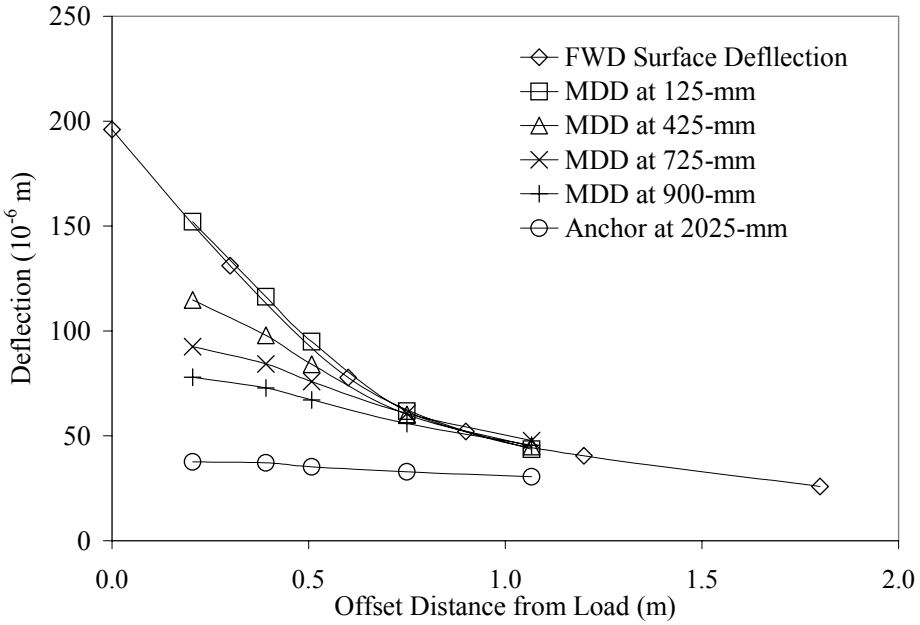

Figure 3. Measured Surface and Depth Deflections on TTI Pavement Section 12

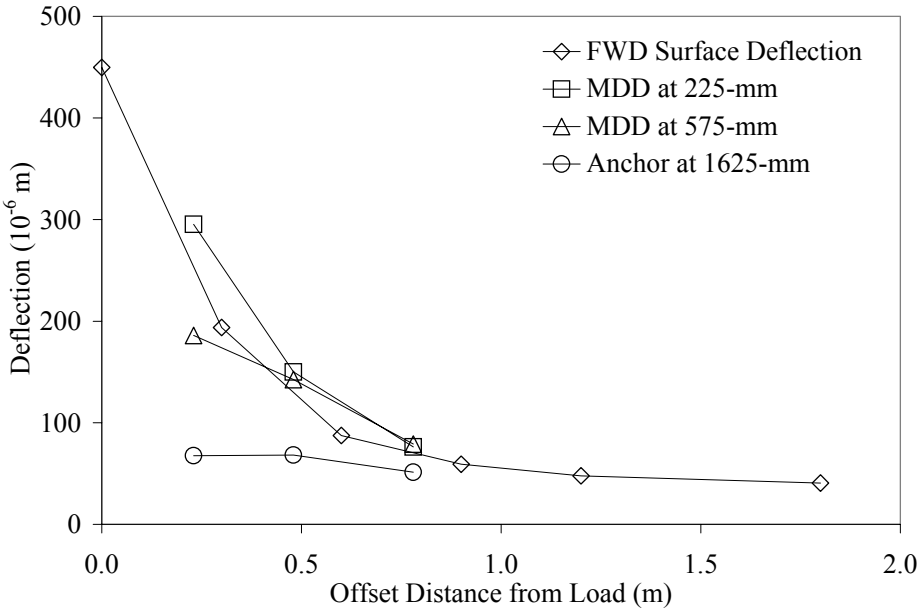

Figure 4. Measured Surface and Depth Deflections on TTI Pavement Section 11

DATA ANALYSIS

In Figure 3, the MDD deflections decrease with depth and are less than the FWD surface deflections in the thick pavement (section 12). In the thin pavement (section 11), the MDD deflections measured within the base layer and subgrade are greater than those measured on the pavement surface (see Figure 4). This indicates that dilation takes place in the granular layers. The dilated material acts like an internal pressure to uplift the surface and push the subbase and subgrade down. Thus, the deflection bowl observed at section 11 cannot be explained by standard linear elastic techniques.

Tables 1 and 3 include absolute surface deflections in micrometers (μm) and normalized surface deflection in μm/kN (deflection per unit load). The deflection per unit load is a good indicator of nonlinear response of the pavement (Uzan and Scullion, 1990). The following observations were made with regard to the absolute and normalized deflections on both pavement sections:

- the absolute deflections (μm) generally increase with increasing load,
- the normalized center deflections (μm/kN) are almost constant in section 12 and decrease with increasing load in section 11, and
- the other normalized deflections (μm/kN) are almost independent of the load.

It is therefore expected that the pavement response is more load-dependent in section 11 than in section 12. Researchers used the surface and depth deflections to backcalculate the material property (moduli) of the pavement layers. Based on the FWD surface deflections and MDD depth deflections, several computer runs were made using the TTI-PAVE finite element program with different material properties until the average percent error in deflections were less than 10 percent The TTI-PAVE runs assumed the surface layer and subgrade to be linearly elastic and the base layer to be nonlinear cross-anisotropic. The base layer was then analyzed as linear isotropic, nonlinear isotropic, and linear cross-anisotropic and the deflections computed were compared to the measured deflection. Tables 5 and 6 summarize the backcalculated material properties used in the finite element program for sections 12 and 11, respectively. The average percent errors of measured deflections are tabulated in Tables 7 and 8 for the material properties considered in the granular layer.

The error values in Tables 7 and 8 suggest that the behavior of unbound granular materials cannot be explained by linear analysis. Nonlinear isotropic and cross-anisotropic material models in the base layer predicted vertical deflections that are close to field deflections in the analyzed TTI pavement sections 11 and 12.

Table 5. Backcalculated Material Properties for TTI Pavement Section 12

Material	Pavement Layer			
Property	HMA	Base	Subbase	Subgrade
k_1	138,000	5860	5170	2070
k_2	0.000	0.255	0.255	0.000
k_3	0.000	0.255	0.255	0.000
n	1.00	0.50	0.50	1.00
m	0.35	0.30	0.30	0.35
μ	1.00	1.50	1.50	1.00

Table 6. Backcalculated Material Properties for TTI Pavement Section 11

Material	Pavement Layer			
Property	HMA	Base	Subbase	Subgrade
k_1	69,000	4480	5170	1930
k_2	0.000	0.255	0.255	0.000
k_3	0.000	0.255	0.255	0.000
n	1.00	0.50	0.50	1.00
m	0.35	0.30	0.30	0.35
μ	1.00	1.50	1.50	1.00

Table 7. Average Percent Errors of Deflections for TTI Pavement Section 12

Base Layer Material Model	Average % Error in	
	FWD	MDD
Linear Isotropic	39.9	35.7
Linear Anisotropic	34.6	38.6
Nonlinear Isotropic	4.8	10.1
Nonlinear Anisotropic	6.3	4.4

Table 8. Average Percent Errors of Deflections for TTI Pavement Section 11

Base Layer Material Model	Average % Error in	
	FWD	MDD
Linear Isotropic	48.6	41.9
Linear Anisotropic	47.2	41.0
Nonlinear Isotropic	6.6	7.0
Nonlinear Anisotropic	4.9	7.8

GEORGIA TECH TEST SECTIONS

The resilient response of five well instrumented full-scale test sections is calculated in this section using the GT-PAVE FE program to validate the anisotropic characterization of UABs and to determine if cross-anisotropic models are practical for routine use to give good results. These test sections, which consisted of three conventional sections with granular bases and two inverted sections with cement stabilized subbases, were a part of an earlier full-scale pavement test study to evaluate factors affecting crushed stone base performance (Barksdale and Todres, 1983). The sections had extensive instrumentation done in the layers to measure a total of eight response parameters, stresses and strains at different pavement locations together with surface deflections.

The important features of the GT-PAVE finite element program, such as nonlinear analysis procedure, incremental loading, and pre-and post-processing capabilities, are discussed first for the classical continuum representation of the granular base layer. Next, the GA Tech full-scale test pit study is briefly described. The results on the laboratory evaluation of the Norcross crushed stone at the University of Illinois are presented. Finally, the resilient responses are predicted at different locations in the test sections considering several methods of UAB characterization for comparison and field validation. These include:

(1) a linear elastic, isotropic analysis,
(2) a linear elastic, cross-anisotropic analysis,
(3) a nonlinear, stress sensitive isotropic analysis,
(4) characterization of the vertical resilient modulus as nonlinear stress sensitive according to a Uzan type model and then assuming that the horizontal modulus is some percentage of the vertical modulus (Tutumluer, 1995),
(5) a nonlinear stress sensitive cross-anisotropic analysis using modulus models developed following the laboratory SID approach (Adu-Osei et al., 2000), and
(6) a nonlinear stress sensitive cross-anisotropic analysis with model parameters obtained from a simplified procedure that uses AASHTO T294-94 resilient modulus test results and adopted earlier by Tutumluer and Thompson (1998).

GT-PAVE FINITE ELEMENT PROGRAM

The GT-PAVE finite element program employs the small-displacement theory and considers the cross-anisotropic behavior exhibited by unbound aggregates when used in a base (Tutumluer, 1995; Tutumluer and Barksdale, 1995). It models flexible pavements as axisymmetric solids consisting of either linear or nonlinear elastic layers. The wheel load is approximated by a circular uniform static load. The program also permits incremental loading in the nonlinear analysis, handles residual compaction stresses. The program does not consider a dynamic analysis and hence neglects inertia forces.

Written in Fortran 77, the GT-PAVE nonlinear finite element program runs on a personal computer and the wheel load is applied in 10 increments. Gravity loading due to self-weight and initial lateral stresses locked in the granular base due to compaction is also considered initially for a more realistic representation of the pavement problem. Pre-processing capabilities include automatic rectangular mesh generation and simple data input. A new post-processor/graphical visualization software package has been adopted for use with the GT-PAVE program. In addition, for improving FE inputs and ease in the modeling efforts, an MS Visual Basic™ user interface has been developed for the program. Post-processing uses Tecplot software version 8.0 (Amtec Engineering Inc., Bellevue, WA) for full output data visualization capability.

The GT-PAVE program solves layered elastic pavement problems using the 8-node quadrilateral elements. Ten different material types can be used with material properties entered for either isotropic (M_R, ν) or cross-anisotropic (M_R^r, ν_r, M_R^z, ν_z, G_R) analysis. Loading types consist of nodal point loads, uniform pressure (edge) loads, gravity loads, and temperature loads. Program development gives emphasis to realistic nonlinear material modeling using both standard and nonstandard laboratory tests, such as the AASHTO T294-94 and the new ICAR testing protocol for anisotropic characterization. Resilient modulus models, such as the K-theta (Hicks and Monismith, 1971), Uzan (1985), UT-Austin (Pezo, 1993), and the bilinear subgrade model (Thompson and Elliot, 1985), which consider both confinement and shear stress effects for the nonlinear behavior of base and subgrade layers, were carefully chosen to be suitable for practical design use. In addition, for the cross-anisotropic characterization of the granular layers, (Uzan 1985) type-stress sensitive models can be assigned for the three moduli, M_R^r, M_R^z, and G_R.

Material nonlinearity is handled by using a secant chord modulus, which was found to be the most effective method of analysis when used with the simplified material models.

The overall nonlinear analysis performed consists of two major parts: (1) first the computation of initial stresses due to overburden including the effects of horizontal residual compaction stresses and then (2) the application of the uniform circular wheel loading at the centerline in the axisymmetric mesh. The gravity and the wheel loadings are, unless specified otherwise, applied in 5 and 10 increments, respectively, until the full load for each is applied in the last increment. The first load increment of the gravity loading is solved assuming linear elastic response. To obtain convergence for nonlinear problems, the number of load increments can be varied to suit the requirements of the problem. The gravity loading including the effects of initial compaction stresses provides a correct starting point with appropriate stress state determined before superposition of the wheel loading.

During each load increment, GT-PAVE computes the resilient response through iterations until correct nonlinear material modeling is achieved. New values of resilient moduli are calculated from the previously computed principal stresses using the modulus models (Uzan, 1985; Pezo, 1993). The new and the old moduli are compared for convergence of the nonlinear iterations using both a cumulative and an individual error criterion. In the full anisotropic characterization option with three Uzan-type models assigned for the vertical, horizontal, and shear moduli, the vertical moduli control convergence of the nonlinear iterations.

Nonlinear Solution Technique

A direct secant stiffness approach was developed for the nonlinear analysis of granular base and subgrade layers and included in the GT-PAVE finite element program. An iterative procedure, which considers a secant stiffness approach, was found to be necessary in the analysis with an incremental loading scheme. The direct secant method gives good convergence of the iterations (see Figure 5). The nonlinear iterations are performed using the appropriate resilient modulus models to calculate the correct vertical resilient modulus corresponding to the total

stress state. The nonlinear analysis is performed using both an incremental loading scheme and an iterative solution technique for each load increment as follows:

1. First the finite element mesh is generated to give the desired pavement geometry. Necessary material property constants, number of load increments, and convergence criteria are input along with initially assumed material properties and the wheel loading.
2. The nonlinear analysis is begun by applying in typically five load increments just the gravity (body weight) loads and the initial residual compaction stresses. For each increment of body loading, principal stresses are calculated at the nine integration points in each element. New values of the secant resilient modulus are computed at each integration point using the material model and the latest principal stresses.
3. To converge smoothly for each load increment as shown in Figure 5a, a damping factor λ, which has values between 0 and 1, was developed to obtain an improved estimate of the resilient modulus for the next iteration in the form:

$$M_R^j = (1-\lambda)\ M_R^{j-1} + \lambda\ M_{R_{Model}}^j \qquad (2)$$

where M_R^j = actual M_R to be used at the end of iteration number j,

M_R^{j-1} = M_R used at the end of iteration number (j-1),

$M_{R_{Model}}^j$ = M_R computed from the model at the end of iteration number j.

The λ values needed for quick convergence were found to be generally between λ = 0.3 and 0.4 especially for wheel loading. Often this λ parameter has to be lowered for achieving convergence.

4. The convergence criteria used consist of (i) a maximum of a 5 percent difference between the old and new values of resilient modulus at each integration point in each element and (ii) a 0.2 percent maximum cumulative error (E_c) criterion:

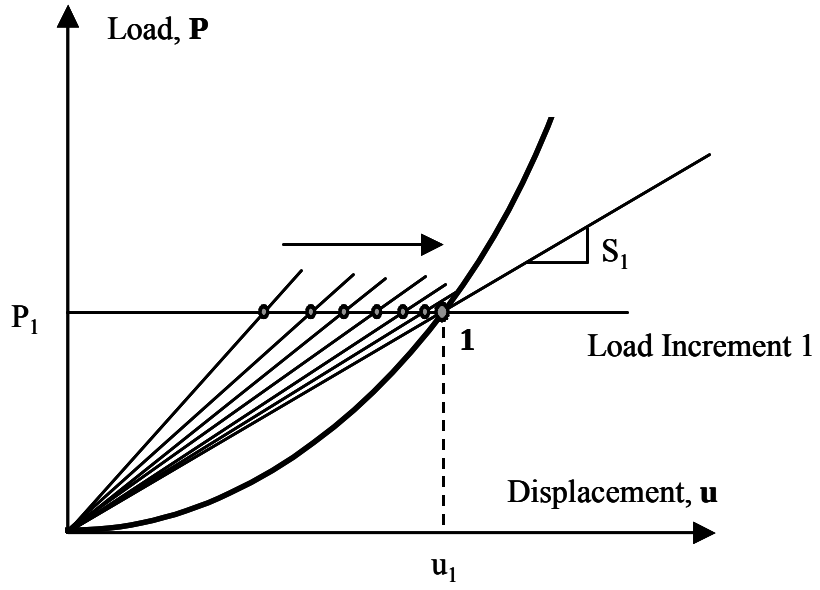

(a) Nonlinear iterations for convergence during load increment 1.

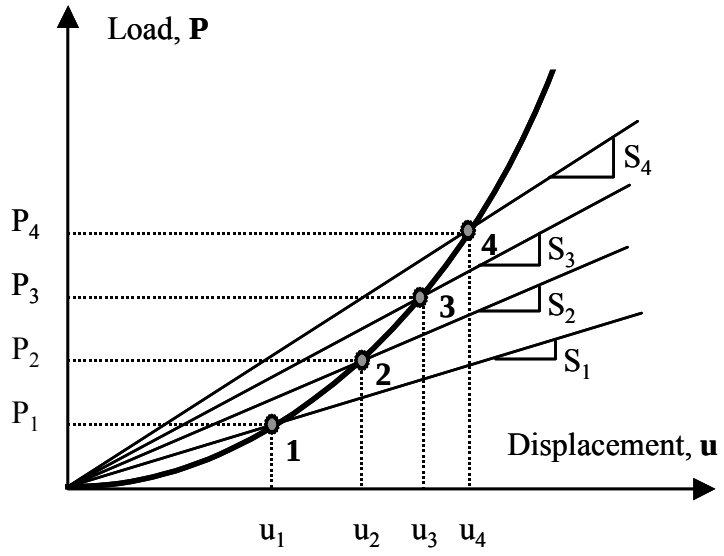

(b) Secant stiffnesses after 4 load increments.

Figure 5. Resilient Modulus Search Technique Using Secant Stiffness for the Stress Hardening Granular Material Behavior

$$E_c = \sum_{i=1}^{n} \left(M_R^j - M_R^{j-1}\right)^2 \Big/ \sum_{i=1}^{n} \left(M_R^j\right)^2 \qquad (3)$$

where n = total number of integration points in the mesh,

j = the last iteration number for each load increment.

5. After the full body weight and residual stresses have been applied and convergence achieved, the wheel load is added in increments permitting the resilient modulus to gradually change as the stresses increase. Typically 10 load increments are used. For each load increment, new values of the secant moduli are computed at each integration point using the most recently calculated stresses in the elements. Once again the moduli for the next iteration are computed using the damping factor λ and checked for convergence.

In general, the cumulative error limit of 0.2% is quite easily satisfied within two iterations. The 5 percent individual error criterion usually controls convergence with up to 7 or 8 iterations being necessary as the wheel loading is gradually increased to the full value.

GEORGIA TECH FULL-SCALE PAVEMENT TEST STUDY

A total of twelve large-scale pavement test sections were tested to evaluate pavement performance (Barksdale and Todres, 1983). Pavement testing was conducted in a facility consisting of a test pit 8 ft. (2.4 m) by 12 ft. (3.6 m) and 5 ft. (1.5 m) deep. A heavy steel reaction frame was constructed over the test pit and an air-over-oil pneumatic loading system was attached to the load frame. Pavements tested in this facility consisted of two inverted sections, five conventional sections having crushed stone bases, and five full-depth asphalt concrete sections (see Table 9). The pavement test sections were fully instrumented with pressure cells and bison type strain coils. The instrumented sections were then tested to either a rutting or fatigue type failure under a repetitively applied, 6,500 lb. (28.9 kN) uniform circular load having a diameter of 9.1 in. (231 mm).

Table 10 summarizes the aggregate gradations and the material properties used in the full-scale test sections. A Georgia DOT B-binder asphalt concrete was employed for the AC surfacing with an AC-20 viscosity grade asphalt cement used in the mix. The standard aggregate base course consisted of crushed granitic gneiss obtained from the Norcross Quarry of Vulcan Materials Co. and prepared by blending in a small 0.125 yd^3 (0.096 m^3) Barber-Greene pugmill 20 percent by weight of No. 5 size aggregate, 25 percent of No. 57, and 55 percent of No. 810 stone sizes. A low to moderate strength micaceous nonplastic silty sand subgrade, classified as an AASHTO A-4 soil, was used beneath the test sections.

Table 9. The Geometry and Performance Summary of Georgia Tech Pavement Test Sections (after Barksdale and Todres, 1983)

Section No.	Asphalt Concrete Thickness (in.)	Crushed Stone Thickness (in.)	Repetitions to Failure	Failure Mode	Comments
CRUSHED STONE BASE					
1	3.5	12.0	3,000,000 3,500,000	Fatigue/ Rutting	Tested to 2.4 million repetitions Failure Extrapolated
2	3.5	8.0	1,000,000	Rutting	
FULL DEPTH ASPHALT					
3	9.0	None	10,000,000	Rutting (1 in.)	Bad Asphalt: AC Content: 5.9 % Flow: 15.4 (1/100 in.)
4	6.5	None	10,000	Rutting (1 in.)	Stability: 1870 lb. Dry Density: 145.1 pcf
5	9.0	None	130,000	Rutting	Rutting Primarily in AC
6	6.5	None	440,000	Rutting	Rutting Primarily in AC
7	7.0	None	150,000	Rutting	
CRUSHED STONE BASE					
8	3.5	8.0	550,000	Rutting	
9	3.5	8.0	2,400,000	Fatigue	Permanent Deformation: 0.28 in.
10	3.5	8.0	2,900,000	Fatigue	Permanent Deformation: 0.34 in.
INVERTED SECTIONS					
11	3.5	8.0	3,600,000	Fatigue/ Rutting	6.0 in. Soil Cement Subbase
12	3.5	8.0	4,400,000	Fatigue/ Rutting	6.0 in. Cement Stabilized Subbase

Note: 1in. = 25.4 mm; 1 psi = 6.895 kPa; 1 lb. = 4.448 kN

Table 10. Aggregate Gradations and Material Properties Used in Flexible Pavement Test Sections

SIEVES	Cumulative % Passing By Weight										Maximum Density (pcf)	Opt. Water Content (%)
	1.5 in. (38 mm)	1 in. (25 mm)	3/4 in. (19 mm)	1/2 in. (13 mm)	3/8 in. (10 mm)	No. 4 (4.75 mm)	No. 10 (2.00 mm)	No.40 (.425 mm)	No. 60 (0.25 mm)	No. 200 (.075 mm)		
AC Aggregate Gradation:(2)	100	100	100	86	75	51	36	18	14	7	147	-
Base Aggregate Gradations:												
No. 5	100	96	37	5	2	-	-	-	-	-	-	-
No. 57	100	98	82	43	20	3	-	-	-	-	-	-
No. 810	100	100	100	100	100	77	56	27	19	8	-	-
Combined	100	99	83	67	61	43	31	15	10	4	137(5)	5.7
Subgrade Gradation:(3)	100	100	100	100	100	100	99	85	70	39	105(4)	18.5
CEMENT STABILIZED SUBBASE PROPERTIES :												
A. Soil - Cement Subbase: 5% by weight of Type I Portland cement added to the silty sand subgrade. (Section 11) Average 28-day unconfined compressive strength = 214 psi.											107(5)	18.0
B. Aggregate - Cement Subbase: 4.5% by weight of Type I Portland cement added to the Combined base. (Section 12) Average 28-day unconfined compressive strength = 1146 psi.											138(5)	6.0

Notes:
1. 1 in. = 25.4 mm; 1 psi = 6.895 kPa; 1 lb = 4.448 kN; 1 pcf = 0.157 kN/m^3
2. The B-binder AC had a 5.2% optimum asphalt content, 4 % voids in the total mix, Marshall mix stability of 2300 lb. (10.2 kN), and a flow value of 9.0/100.0 in. (2.3 mm).
3. Maximum aggregate size = 1.5 in. (38 mm)
4. Determined by AASHTO T-99 test method
5. Determined by AASHTO T-180 test method

Test Section Construction

The silty sand subgrade was placed in the pit in 2 -in. (51 mm) lifts up to a total thickness of 50 in. (1270 mm) in the conventional sections and 44 -n. (1118 mm) in the inverted sections. Each lift was compacted using a Wacker or a Jay compactor to 98 percent of AASHTO T-99 standard Proctor maximum dry density at a moisture content of 20.5 percent. A spring loaded static penetrometer was used to insure the uniformity of the subgrade during construction. The as constructed density was determined using a thin wall, drive tube sampler.

The 6-in. (152-mm) thick cement stabilized subbase used only in the inverted sections was constructed on top of the subgrade followed by the placement of the crushed stone base. All base and subbase layers were placed in approximately 2-in. (51 mm) lifts. Compaction of the subbase and base was achieved using 5 to 7 passes of the Jay 12 vibrating plate compactor. The unstabilized aggregate bases were compacted to 100 percent of the AASHTO T-180 modified Proctor maximum dry density. Nuclear density measurements revealed that due to the presence of the underlying rigid cement stabilized subbase, the compaction density in the unstabilized aggregate base of the inverted sections was 105 percent of the T-180 maximum dry density.

The cement-stabilized layers used in the inverted sections were allowed to cure for 28 days before loading the test sections. The B-binder asphalt concrete mix was placed over the unstabilized base. This mixture was used to give a strong asphalt concrete surface course so as to resist rutting in that layer under the heavy applied loading.

Performance of the Test Sections

The full-scale laboratory tests conducted to failure permitted comparing the performance of the conventional sections with both the inverted sections and the full depth asphalt concrete sections (see Tables 9 and 11). A maximum rut depth of 0.5 -in. (13 mm) was considered to constitute a rutting failure. A fatigue failure of the sections was also considered to occur when the surface cracks became connected together to form a grid type pattern, usually over the loaded area. Only hairline cracks were allowed to develop. Before wider cracks formed, testing was

terminated because of the large number of load repetitions required to reach this state of deterioration.

Overall, the two inverted sections performed the best of all the sections studied (see Table 9). Both inverted sections (section 11 and 12) failed in combined rutting and fatigue with the strongest cement stabilized crushed stone subbase (section 12) withstanding up to a maximum of 4.4 million load repetitions. The two inverted sections also exhibited lower vertical stresses on the subgrade and lower resilient surface displacements than the others (see Table 11).

Table 11 presents a detailed summary of the observed resilient response of the pavement test sections as obtained at different locations in the sections. In addition to the critical response values such as the vertical stress on the subgrade and the horizontal tensile strain at the bottom of the asphalt concrete (AC), up to 7 more response variables (stresses, strains and displacements) were measured in the sections using the bison type strain coils and pressure cells. Researchers used these results in this study to compare the predicted with the observed resilient response of the test sections using the GT-PAVE nonlinear finite element program. The accuracy of the overall modeling of resilient behavior of both the conventional and inverted sections is related to how well the measured response variables are predicted at the same time.

LABORATORY EVALUATION OF NORCROSS CRUSHED STONE AT THE UNIVERSITY OF ILLINOIS

In summer of 2001, the aggregate material used in the granular base layers of the GA Tech pavement test sections, a granitic gneiss referred to in this report as the Norcross crushed stone, was obtained from the Norcross, Georgia Quarry of Vulcan Materials Co. Laboratory testing of the aggregate samples was conducted at the University of Illinois as part of the ICAR 502 project activities. The primary goal was to establish the stress sensitive, cross-anisotropic model parameters for the Norcross crushed stone from resilient modulus testing using an advanced IPC triaxial testing device, the University of Illinois FastCell (UI-FastCell), and to be

Table 11. Detailed Summary of Resilient Test Section Response

Section	Horizontal Tensile Strain (micro in./in.)		Vertical Stress (psi)		Vertical Strain (micro in. /in.)				Surface Deflection (in.)	
	Bottom AC	Bottom Base	Top Base	Top Subgrade	AC	Top Base	Bottom Base	Top Subgrade	10 in. from Centerline	14.5 in. from Centerline
CRUSHED STONE BASE										
1	465	597	-	3.4	-	-	-	1700	0.03	0.015
2	674	754	-	-	11000	21300	-	13100	0.019	0.01
FULL DEPTH ASPHALT										
3	Premature Failure - Excessive Asphalt Content									
4	Premature Failure - Excessive Asphalt Content									
5	319	-	-	8.7	850	-	-	1380	0.012	0.007
6	460	-	-	12.6	-	-	-	1500	0.02	0.012
7	410	-	-	12.9	650	-	-	2200	0.019	0.013
CRUSHED STONE BASE										
8	300	375	-	11.9	-	560	110	1850	0.02	0.013
9	280	1080	62	11.1	-	560	340	1750	0.022	0.013
10	400	1025	54	6.8	-	620	400	2500	0.017	0.01
INVERTED SECTION										
11	340	54	-	3.3	-	730	370	390	0.007	0.003
12	260	22	-	3.4	-	760	420	340	0.006	0.003

Note: 1. A "-" in a data field indicates data was not taken.
1 in = 25.4 mm; 1 psi = 6.895 kPa; (Compression is positive)

able to validate the effectiveness of the anisotropic UAB modeling approach undertaken in the ICAR 502 project.

Description and Capabilities of the UI-FastCell

University of Illinois FastCell is an advanced laboratory-testing device that was custom-designed and manufactured a few years ago based on the latest research findings (Tutumluer and Thompson, 1997a and 1997b). UI-FastCell has provisions for measurement of on-sample vertical and radial displacements as well as pulsing of the major principal stress in the vertical or radial direction by the use of the two independently controlled stress channels. Since it is not possible to reorient the granular samples in the triaxial cell, applying and switching of the various stress states on the same specimen facilitates determining especially the load-induced anisotropy. The device is suitable for performing aggregate tests following the ICAR protocol, which uses three stress regimes and ten stress levels within each regime to determine stress sensitivity and cross anisotropy. The device is also suitable for simulating field stress conditions in the laboratory and for studying the effects of principal stress rotation due to moving wheel loads that involve a change in total shear stress direction.

UI-FastCell uses a fluid/air interface to minimize compressibility effects when conducting tests with mandatory horizontal stress cycles. This is useful for investigating anisotropic effects and the response to loading in which a 90° rotation of planes of principal stress is important. Figure 6a shows a picture of the UI-FastCell with the confinement cell lowered onto the specimen for the testing position. An air actuator applies the axial pressure and the confining pressures are cycled through a hydraulic fluid within the rubber membrane. The driving cylinders on the back of the confining cell (not shown here) include an air-fluid interface, which provides fast application and switching of the dynamic loading. Figure 6b presents a drawing of the cylindrical specimen, approximately 6-in. in diameter by 6-in. high under the independently applied vertical and radial stresses and the instrumentation consisting of LVDTs measuring axial and radial specimen deformations.

Material Properties

Moisture-density tests were conducted at the University of Illinois upon receiving the Norcross crushed stone samples. Table 12 compares the modified Proctor (AASHTO T-180) maximum dry densities and the optimum moisture contents of the Norcross stone and other GA Tech base course materials, i.e., the standard, fine, and coarse gradation materials, reported previously by Barksdale and Todres (1983). The Norcross aggregate tested has a higher maximum dry density than those of the standard and fine aggregates as shown in Table 12. The optimum moisture content is also higher than the reported percentages for the other materials. These discrepancies necessitated sieve analysis tests to be performed on the Norcross stone to determine its gradation properties.

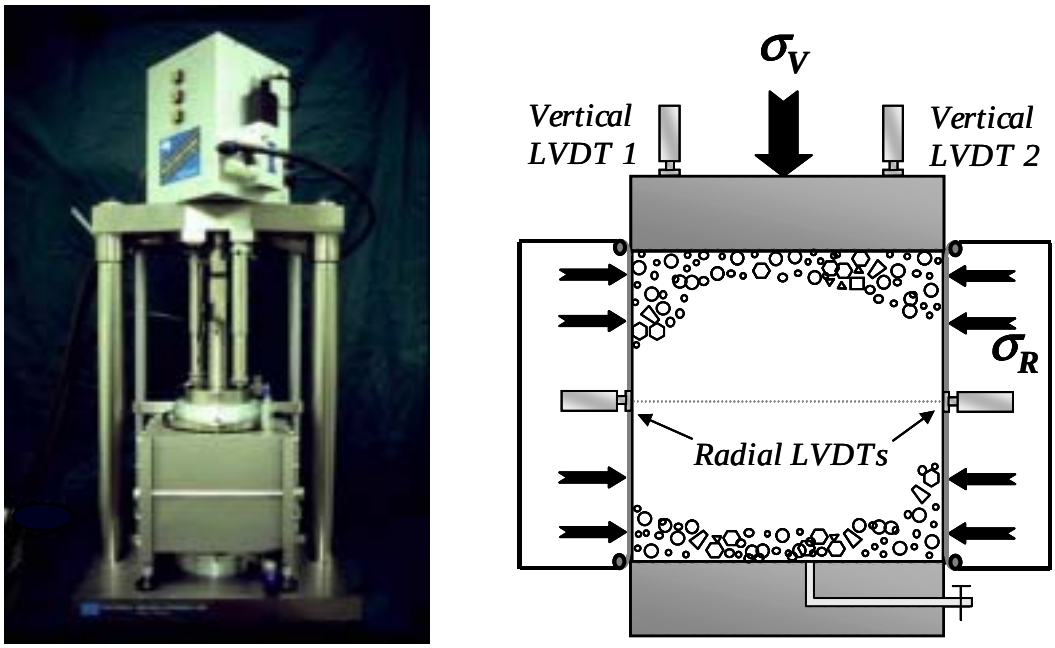

(a) Photograph showing the UI-Fastcell (b) Representation of the cylindrical specimen

Figure 6. The University of Illinois FastCell Triaxial Testing Device

Figure 7 shows gradation curves for the Norcross crushed stone and other GA Tech base course aggregates with top sizes varying from 1 in. to 1.5 in. Tests number I, II, and III refer to a total of 3 sets of modulus tests performed in this study on the Norcross aggregate at different material properties. Tests I and II were conducted without changing the original gradation of the material, i.e., as received from the Norcross Quarry. This original gradation, however, had an 8 percent fines content (minus 0.075 mm or No. 200 sieve) considerably higher than the 4 percent maximum fines allowed in the "Standard" gradation primarily used in the GA Tech test section base courses. Therefore, not only the amount of fines had to be reduced down to 4 percent but also the exact same gradation of the "Standard" material had to be engineered for the Norcross crushed stone when preparing the Test III samples. As clearly shown in Figure 7, the final gradation for Test III samples is identical to that of the "Standard" gradation material.

Table 12. Modified Proctor (AASHTO T-180) Properties of Georgia Tech Base Course Aggregates

Material Gradation	Maximum Dry Density (pcf)	Maximum Dry Density (Kg/m^3)	Optimum Moisture Content (%)
Standard	137.0	2,217	5.7
Fine	139.5	2,257	6.8
Coarse	141.5	2,289	6.8
Norcross Crushed Stone	*140.2*	*2,268*	*7.1*

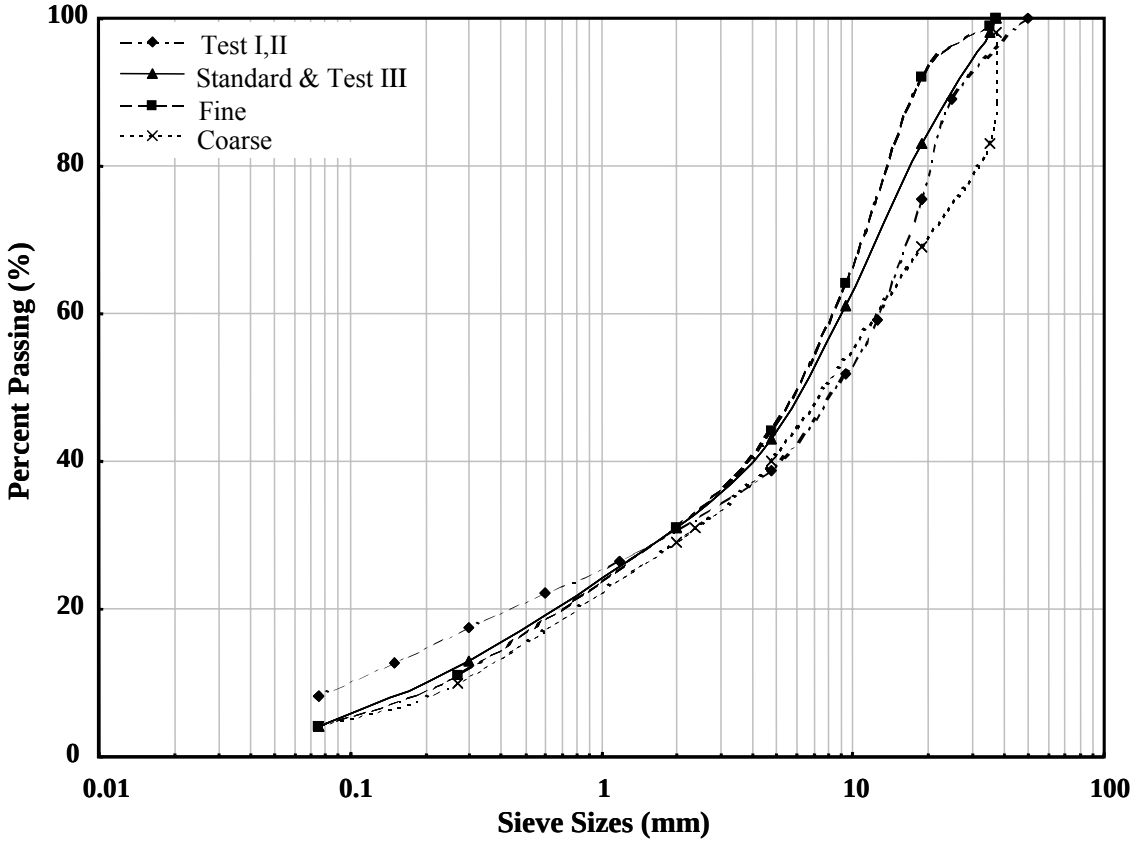

Figure 7. Gradation Curves for Norcross Crushed Stone and Other GA Tech Base Materials

The achieved dry densities and moisture contents are listed in Table 13 for all the samples prepared for three sets of modulus tests. Samples prepared for Test series I and II were tested at moisture-density states very close to the optimum moisture content and the maximum dry density obtained for the original gradation Norcross crushed stone. On the other hand, samples for Test series III were tested at a much lower achieved moisture content of 4.7 percent, comparable to the 5.7 percent optimum moisture content of the "Standard" gradation aggregate, and at a somewhat higher achieved dry density of 142.3 pcf. As a result, the material properties of Test III samples are more representative of the standard high quality UAB courses constructed and tested at the GA Tech test pit facility.

Table 13. Achieved Dry Densities and Moisture Contents for All Modulus Test Samples

	Achieved Moisture Content (%)	Achieved Dry Density (pcf)	% Fines Content
Test I	7.5	139.6	8
Test II	7.1	140.2	8
Test III	4.7	142.3	4

Resilient Modulus Testing

Researchers performed three sets of modulus tests, I, II, and III, on the Norcross crushed stone samples using the UI-FastCell and following each of the two procedures, the standard AASHTO T294-94 and the ICAR test protocol developed by Texas A&M researchers (Adu-Osei et al., 2000). For each test, cylindrical specimens, 6-in. in diameter by 6-in. high, were prepared by compacting with a pneumatic vibratory compactor. This modified Proctor compaction effort on the specimens was assumed to represent the initial conditions of the GA Tech granular base layers just after pavement construction. Therefore, the specimens were not conditioned before the actual testing sequence. Following the standard AASHTO T294-94 procedure, test subjected the specimens to 15 triaxial stress states that are typically less severe than the failure stress states. A haversine load waveform was applied with a load pulse duration of 0.1 seconds (10-Hz), and a rest period of 0.9 seconds. Following the ICAR test protocol, three stress regimes, triaxial compression, extension, and pure shear loading, applied ten stress levels within each regime to determine the three cross anisotropic moduli and two Poisson's ratios. In addition, one other modulus test following the AASHTO T294-94 procedure was also performed on a 6-in. in diameter by 12-in. high standard triaxial specimen having Test series III material properties. The purpose of this last test was to later implement in anisotropic modeling a simplified procedure proposed by Tutumluer and Thompson (1998).

Figure 8 shows for each test sample variations of the vertical resilient modulus with increasing deviator stresses obtained following the AASHTO T294-94. The moduli were computed by dividing the applied vertical deviator stress by the recoverable strain measured in

the vertical direction. Overall, the moduli increased as the applied confining stresses increased. At each confining pressure, i.e., 3, 5, 10, 15, and 20 psi, the vertical moduli obtained from samples with the Test III material properties were much greater than the moduli obtained from samples having the original Norcross crushed stone gradation with 8 percent content.

Similar trends in the vertical modulus behavior were obtained from tests conducted following the ICAR test protocol. Table 14 and Figure 9 present K-θ modeling (Hicks and Monismith, 1971) results for the vertical moduli obtained from samples tested following the ICAR test protocol and the AASHTO T294-94 for the 6-in. in diameter by 12-in. high standard triaxial specimen. The modulus curves shown in Figure 8 labeled as Texas-1 to Texas-3 correspond to the vertical modulus models obtained from samples having material properties from Tests I to III and running the ICAR test protocol in the laboratory. Similar to Figure 8, these curves also indicate that the highest modulus values were obtained from the sample having Test III material properties with only 4 percent fines allowed in the gradation. The Texas-3 model produces moduli even higher than the values obtained for the 6-in. in diameter by 12-in. high specimen tested at the same material properties following the T294-94 procedure.

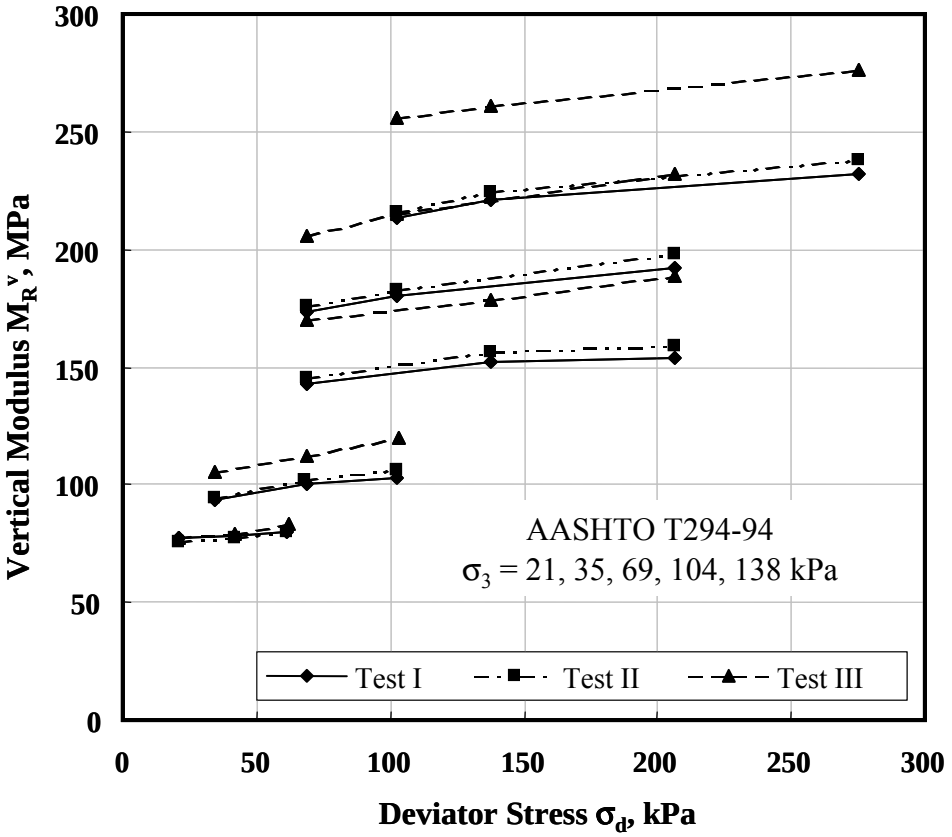

Figure 8. Variation of Vertical Moduli with Deviator Stresses from AASHTO T294-94 Tests

Table 14. Model Parameters for Vertical Moduli: ICAR Protocol and AASHTO T294-94 Tests

K-θ Model: $M_R = K * \theta^n$		
Model	K (psi)	n
Texas-1	3581.98	0.621
Texas-2	2085.04	0.731
Texas-3	5928.80	0.553
T294-94 procedure -3	6989.25	0.427

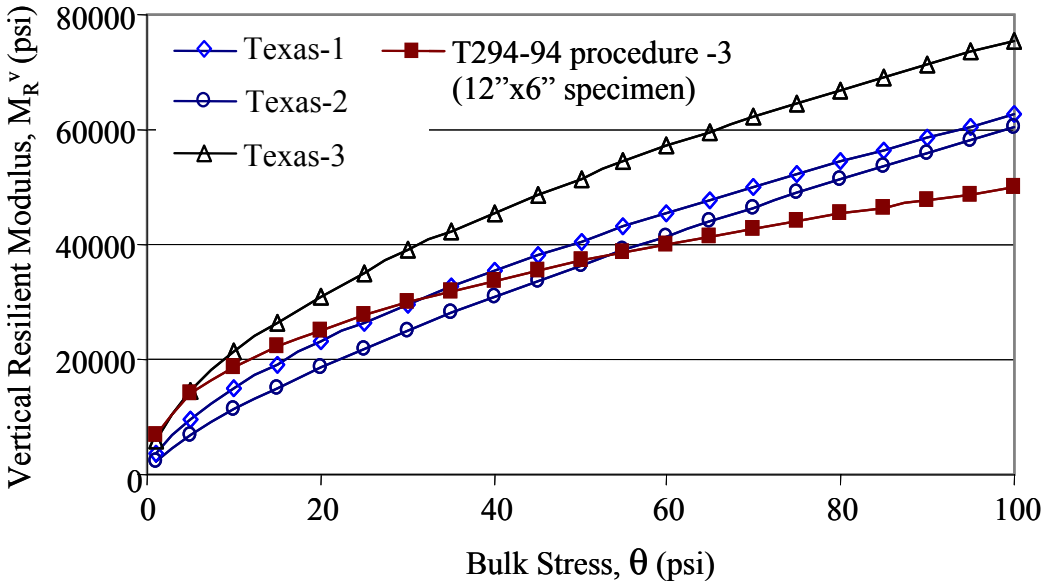

Figure 9. K-θ Models Showing Variation of Vertical Moduli with Bulk Stresses

MODELING OF GA TECH PAVEMENT TEST SECTIONS

Two types of GA Tech flexible pavement sections are primary candidates for analysis: 1) conventional sections with a granular base but no subbase and the inverted sections having an unstabilized crushed stone base sandwiched between a lower cement stabilized subbase 2) the upper asphalt concrete surfacing. Figure 10 shows the typical cross sections used for the conventional (sections 8, 9, and 10) and inverted sections (sections 11 and 12) along with the locations of the measured and predicted response variables. In both the conventional and the inverted sections, a 3.5-in. (89 mm) AC binder was employed for the surfacing. The unstabilized aggregate base course consisted of the Norcross crushed granitic gneiss 8 in. (203 mm) in thickness. Sections 11 and 12, the inverted sections, had an additional 6 -in. (152 mm) subbase consisting of a cement-stabilized subgrade and stronger cement treated aggregate base, respectively. The thickness of the micaceous silty sand subgrade was 44 in. (1118 mm) in the inverted sections and 50 in. (1270 mm) in the conventional sections. A 6-in. (152 mm) thick concrete slab was located at the bottom of the subgrade.

A 140-element, 475-node axisymmetric GT-PAVE finite element mesh analyzed both the conventional and inverted sections as elastic layered systems. To model the test sections, the

wheel load was applied as a uniform pressure of 100 psi (689 kPa) over a circular area of radius 4.55 in. (116 mm) (see Figure 10). A fixed boundary was assumed at the bottom of the subgrade where the concrete slab was placed.

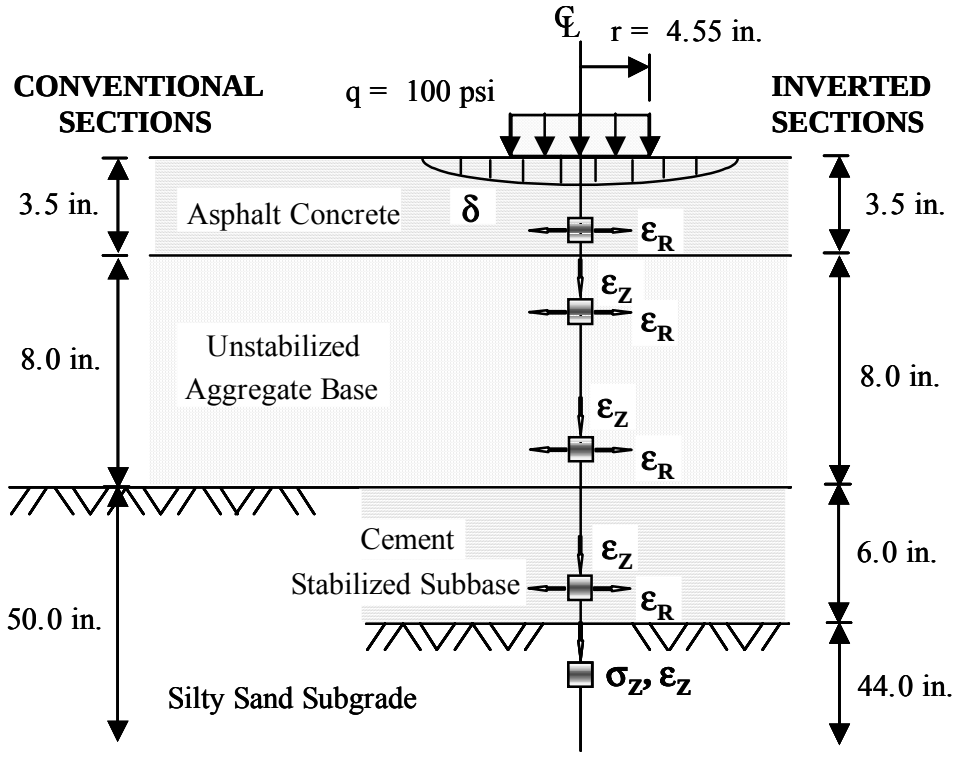

Figure 10. Typical Cross Sections of GA Tech Pavement Test Sections

Material Properties Assigned in the Early Work by Tutumluer (1995)

Nonlinear anisotropic modeling of the GA Tech test section UAB layers was first attempted by Tutumluer (1995) in his PhD thesis study. In this and the following sections, this early work by Tutumluer (1995) will be summarized for the pavement section material properties assigned in the GT-PAVE analyses and the resilient response predictions obtained, respectively. The UAB modeling approach taken was simply the characterization of the vertical resilient modulus as nonlinear stress sensitive according to a Uzan type model and then assuming that the horizontal modulus is some percentage of the vertical modulus (Tutumluer, 1995).

Table 15 summarizes the material properties used by Tutumluer (1995) in the pavement test sections including initial guesses and the model parameters needed for the nonlinear analysis.

The initial guesses consist of the vertical and horizontal values of resilient modulus and Poisson's ratio, vertical shear modulus and material densities. Model parameters are given for the Uzan model (1985) used in the granular base and for the bilinear approximation used in the subgrade (see Table 15). The nonlinear model parameters used in the crushed stone base differed between the conventional and the inverted sections since a higher percentage compaction was achieved in the inverted sections due to the presence of the underlying cement stabilized subbase.

The subgrade and the unstabilized aggregate base were treated as nonlinear elastic materials while the AC surfacing and cement stabilized subbase were modeled as linear elastic materials. In addition, the base was also given cross-anisotropic material properties. The resilient modulus of the AC layer was taken based on previous studies (Barksdale et al., 1989) to be 250 ksi (1720 MPa) with a corresponding Poisson's ratio of 0.35. A modulus of 600 ksi (4,140 MPa) was assumed in the cement treated silty sand subbase of Section 11, and a modulus of 1,500 ksi (10,340 MPa) was used for the cement stabilized crushed stone subbase of Section 12. Both sections used a Poisson's ratio of 0.2.

When modeling the pavement sections, researchers divided both the nonlinear aggregate base and the subgrade into sublayers, thus enabling a more realistic assignment of initial material properties (see Table 15). The unstabilized crushed stone bases were initially assigned vertical resilient moduli varying from 30 ksi (206.9 MPa) at the bottom to 60 ksi (413.7 MPa) at the top. The horizontal resilient moduli were initially assumed to be 80 percent of the vertical moduli at the top of the anisotropic base. In the conventional sections only, the horizontal moduli were initially 2 percent of the vertical moduli in the lower portion of the base to account for the horizontal tension. Similarly, an assumed Poisson's ratio of 0.43 in the vertical direction was reduced to 0.15 in the horizontal direction based on previous studies (Barksdale et al., 1989). The subgrade was also initially assigned nonlinear isotropic material properties with a Poisson's ratio of 0.40 and the resilient moduli varying from 3 ksi (20.7 MPa) at the top to 15 ksi (103.4 MPa) at the bottom.

Table 15. Material Properties and Model Parameters Used In Modeling Pavement Test Section response (after Tutumluer, 1995)

Layer Type	Thickness (in.)	Vertical Modulus (psi)	Vertical Poisson's Ratio	Horizontal Modulus (psi)	Horizontal Poisson's Ratio	Shear Modulus (psi)	Model Parameters (3/4) K_4 / K_{10} (psi)	K_5 / K_{11}	K_6 / K_{12}	K_{13}	Density (pcf)
Asphalt Concrete (1)	3.5	250,000	0.35	-	-	-	-	-	-	-	147
Crushed Stone Base: (3)											
Conventional Sections: Top	2.6	53,960	0.43	42,940	0.15	18,867	4,867	0.80	-0.05	-	137
Middle	2.6	38,000	0.43	3,234	0.15	13,287	4,867	0.80	-0.05	-	137
Bottom	2.8	31,084	0.45	863	0.10	10,719	4,867	0.80	-0.05	-	137
Inverted Sections: Top	2.6	53,960	0.43	42,940	0.15	18,867	5,367	0.61	-0.07	-	144
Middle	2.6	38,000	0.43	30,239	0.15	13,287	5,367	0.61	-0.07	-	144
Bottom	2.8	31,084	0.45	24,736	0.10	10,719	5,367	0.61	-0.07	-	144
Cement Stabilized Subbase: (1)											
Soil-Cement (Sect. 11)	6.0	600,000	0.2	-	-	-	-	-	-	-	107
Stone-Cement (Sect. 12)	6.0	1,500,000	0.2	-	-	-	-	-	-	-	138
Silty Sand Subgrade: (4)											
Top	3.0 (2.0 [2])	3,000	0.4	-	-	-	5,900	2.5	11640	26.67	105
Middle	27.0 (22.0 [2])	6,000	0.4	-	-	-	5,900	2.5	11640	26.67	105
Bottom	20.0	15,000	0.4	-	-	-	5,900	2.5	11640	26.67	105

Notes: 1. Isotropic linear elastic analysis
2. Inverted sections only
3. Cross-anisotropic nonlinear analysis using Uzan's model
4. Isotropic nonlinear analysis using bilinear representation
5. 1 in. = 25.4 mm; 1 psi = 6.895 kPa; 1 pcf = 0.157 kN/m^3

Uzan's model:

$$M_R = K_4 \left(\frac{\theta}{P_0}\right)^{K_5} \left(\frac{\sigma_d}{P_0}\right)^{K_6}$$

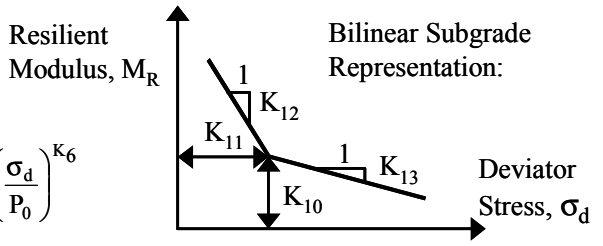

Test Section Resilient Response Predictions by Tutumluer (1995)

Table 16 compares the eight measured resilient response variables with the values predicted by Tutumluer (1995) from his early work. The average values of the measured resilient response of the conventional sections, sections 8, 9, and 10, were used in the comparisons. In general, finite element predictions were found to be in reasonably good agreement with the observed behavior of both the conventional and inverted sections. The predicted values of surface deflections, vertical strain and stress on the subgrade, and radial strains at the bottom of base and AC are essentially the same as the measured ones in the conventional sections. In inverted sections, predicted vertical and radial strains in different layers were in better agreement with observed response for section 11 than for section 12. The vertical stress on top of subgrade was, however, predicted better in section 12 than in section 11. The vertical strains on top of the base could not be predicted to a high degree of accuracy.

The UAB modeling approach taken was simply the characterization of the vertical resilient modulus as nonlinear stress sensitive according to a Uzan type model and then assuming that the horizontal modulus is some percentage of the vertical modulus (Tutumluer, 1995). A 15 percent tension modification factor n (= M_R^h / M_R^v), *which was empirically obtained in the nonlinear analysis by trial and error*, was needed in the bottom portion of the base to obtain good radial strain prediction compared to measured values in the conventional sections. Similarly, a 10 to 20 percent reduction in vertical moduli was also reported by others assigned in horizontal direction in their analyses of cross-anisotropic bases (Chan et al., 1989 and Barksdale et al., 1989).

The predictions summarized by Tutumluer (1995) in Table 16 verified the ability of nonlinear, anisotropic finite element models such as GT-PAVE, to reasonably accurately predict *at the same time* a large number of measured stress, strain, and deflection response variables. It was noted that such predictions are hard to achieve and therefore indicate that the stress sensitive, anisotropic modeling approach used is reasonably valid.

Table 16. Comparison of Predicted and Measured Response Variables (after Tutumluer, 1995)

RESPONSE	TOP SUBGRADE		BOTTOM SUBBASE		BOTTOM BASE		TOP BASE	BOTTOM AC		SURFACE DEFLECTION		
	σ_z (psi)	ε_z (10^{-6})	ε_R (10^{-6})	ε_z (10^{-6})	ε_R (10^{-6})	ε_z (10^{-6})	ε_z (10^{-6})	ε_R (10^{-6})	ε_z (10^{-6})	$\delta_{C.L.}$ [2] (in.)	$\delta_{10"}$ [3] (in.)	$\delta_{14.5"}$ [3] (in.)
MEASURED (Conventional[4])	9.9	2000	-	-	-936	280	580	-330	-	0.028	0.017	0.013
PREDICTED (Conventional)	9.5	2080	-	-	-985	478	626	-384	553	0.026	0.017	0.013
MEASURED (Inverted 11)	3.3	390	-	-	54	370	730	-340	-	0.019	0.007	0.003
PREDICTED (Inverted 11)	4.0	390	-79	45	51	317	1050	-348	536	0.016	0.009	0.006
MEASURED (Inverted 12)	3.4	340	-	-	22	420	760	-260	-	0.016	0.006	0.003
PREDICTED (Inverted 12)	3.5	236	-46	25	35	362	1047	-341	532	0.015	0.008	0.006

Notes:
1. A "-" in data field indicates not applicable or no data was taken
2. Measured deflections at centerline $\delta_{C.L.}$ are extrapolated
3. Deflections measured at 10 in. and 14.5 in. radial distances away from centerline
4. Measured values are averaged from response of Sections 8, 9, and 10
5. 1in. = 25.4 mm; 1 psi = 6.895 kPa; (Compression is positive)

Test Section Response Predictions From Linear Elastic Analyses

For the current validation study, linear elastic analyses were first performed by considering both an isotropic and a cross-anisotropic granular base layer. The AC surfacing and the cement stabilized subbase layers in the inverted sections were assigned the same linear elastic material properties reported previously in Table 15. The subgrade was also assigned linear isotropic material properties with a Poisson's ratio of 0.40 and the resilient moduli varying from 3 ksi (20.7 MPa) at the top to 15 ksi (103.4 MPa) at the bottom.

Table 17 summarizes the isotropic and cross-anisotropic granular base properties, moduli and Poisson's ratios, assigned in modeling the conventional and inverted sections. Three different constant resilient moduli (vertical moduli for anisotropic runs), i.e., 40, 60, and 80 ksi, were considered for analyses. Following the good predictions obtained by Tutumluer (1995), in all anisotropic runs, the horizontal and shear moduli were assumed to be 15 percent and 33 percent of the vertical moduli, respectively.

Table 17. Linear Elastic Base Properties Used In Modeling Pavement Test Section Response

Linear Elastic Analysis		
All Isotropic Runs	M_R = 40,000 psi or 60,000 psi or 80,000 psi	ν = 0.43
All Anisotropic Runs	M_R^v = 40,000 psi or 60,000 psi or 80,000 psi M_R^h = 15% of M_R^v and G = 33% of M_R^v	ν_v = 0.43 ν_h = 0.15

Tables 18 and 19 compare the measured response variables with GT-PAVE predictions for the conventional and inverted sections, respectively. Table 19 lists only the results obtained for the 60-ksi moduli since this value was found to give the best predictions for the conventional sections. In contradiction with the isotropic analysis results, the finite element predictions obtained from the anisotropic analyses are in reasonably good agreement with the observed behavior of test sections. Especially, the predicted values of surface deflections, vertical strain/ stress on subgrade, and radial strains at the bottom of base and AC are very close to the average measured values in the conventional sections. Nonetheless, the vertical strains at the bottom of base in inverted sections could not be predicted to a high degree of accuracy from the isotropic analyses.

Table 18. Comparison of Predicted and Measured Response Variables for Conventional Pavement Sections – Linear Elastic Analyses

Response	Top Subgrade		Bottom Base		Top Base	Bottom AC		Surface Deflection		
	σ_Z (psi)	ε_Z (10^{-6})	ε_R (10^{-6})	ε_Z (10^{-6})	ε_Z (10^{-6})	ε_R (10^{-6})	ε_Z (10^{-6})	$\delta_{C.L.}$ (in)	$\delta_{10"}$ (in)	$\delta_{14.5"}$ (in)
Section 8	11.9	1850	375	110	560	300	-	-	0.02	0.013
Section 9	11.1	1750	1080	340	560	280	-	-	0.022	0.013
Section 10	6.8	2500	1025	400	620	400	-	-	0.017	0.01
Ave. Measured (Conventional)	9.9	2000	-936	280	580	-330	-	0.028	0.017	0.013
Linear Isotropic								$\delta_{C.L.}$ (in)	$\delta_{9.55"}$ (in)	$\delta_{13.55"}$ (in)
M_R = 40 ksi	8.6	1193	-393	697	984	-389	531	0.023	0.015	0.013
M_R = 60 ksi	7.6	1020	-325	562	735	-289	441	0.021	0.014	0.012
M_R = 80 ksi	6.9	904	-278	476	582	-225	384	0.019	0.013	0.011
Linear Anisotropic								$\delta_{C.L.}$ (in)	$\delta_{9.55"}$ (in)	$\delta_{13.55"}$ (in)
M_R^v = 40 ksi	10.8	2112	-953	408	1106	-492	634	0.026	0.017	0.013
M_R^v = 60 ksi	10.2	2000	-907	303	845	-404	556	0.024	0.016	0.013
M_R^v = 80 ksi	9.6	1879	-848	246	691	-342	502	0.023	0.015	0.013

Table 19. Comparison of Predicted and Measured Response Variables for Inverted Pavement Sections – Linear Elastic Analyses

Response	Top Subgrade		Bottom Subbase		Bottom Base		Top Base	Bottom AC		Surface Deflection		
	σ_Z (psi)	ε_Z (10^{-6})	ε_R (10^{-6})	ε_Z (10^{-6})	ε_R (10^{-6})	ε_Z (10^{-6})	ε_Z (10^{-6})	ε_R (10^{-6})	ε_Z (10^{-6})	$\delta_{C.L.}$ (in)	$\delta_{10"}$ (in)	$\delta_{14.5"}$ (in)
Section 11 (Measured)	3.3	390	-	-	54	370	730	-340	-	0.019	0.007	0.003
Section 12 (Measured)	3.4	340	-	-	22	420	760	-260	-	0.016	0.006	0.003
Linear Isotropic										$\delta_{C.L.}$ (in)	$\delta_{9.55"}$ (in)	$\delta_{13.55"}$ (in)
Section 11 M_R = 60ksi	3.81	377	-61	35	14	72	739	-264	431	0.013	0.083	0.074
Section 12 M_R = 60ksi	3.36	310	-36	19	18	77	744	-265	434	0.013	0.008	0.007
Linear Anisotropic										$\delta_{C.L.}$ (in)	$\delta_{9.55"}$ (in)	$\delta_{13.55"}$ (in)
Section 11 M_R^v = 60ksi	3.79	367	-54	32	15	274	942	-289	452	0.015	0.009	0.008
Section 12 M_R^v = 60ksi	3.38	307	-33	18	18	302	950	-290	454	0.014	0.009	0.008

Test Section Response Predictions from Nonlinear Isotropic Analyses

Nonlinear isotropic analyses were next performed by considering an isotropic, stress sensitive granular base layer. The AC surfacing and the cement stabilized subbase layers in the inverted sections were assigned the same linear elastic material properties reported previously in Table 15. The subgrade was, however, treated as a nonlinear elastic material and characterized using the bilinear model (see Table 15).

Table 20 summarizes the isotropic model parameters and the Poisson's ratios used in modeling the granular bases of the conventional and inverted pavement test sections. Except for the previous GA Tech model, the resilient modulus models were developed from the results of various tests conducted at the University of Illinois. Different from the values used by Tutumluer (1995), the Poisson's ratios listed for the three Texas models were the out of plane Poisson's ratios, ν_v, directly obtained from running the SID scheme on the laboratory test results.

Table 20. Isotropic Model Parameters Used In Modeling Pavement Test Section Response

Nonlinear Isotropic Analysis				
Isotropic Runs	Model Parameters†			Poisson's Ratio
	K1	K2	K3	
Previous GA Tech Model	4867	0.80	-0.05	0.43[1], 0.45[2]
Texas Model – 1st Test	4927.9	0.431	0.171	0.11
Texas Model – 2nd Test	3090.2	0.496	0.211	0.12
Texas Model – 3rd Test	7446.5	0.417	0.122	0.08
AASHTO T294-94 (6"×12" specimen)	6606.7	0.498	-0.079	0.43[1], 0.45[2]

[1] Poisson's ratio for top two sub-layers

[2] Poisson's ratio for bottom sub-layer

† $M_R = K1 \times \left(\frac{\theta}{P_0}\right)^{K2} \left(\frac{\sigma_d}{P_0}\right)^{K3}$

Tables 21 and 22 compare the measured response variables with GT-PAVE predictions for the conventional and inverted sections, respectively. In general, the finite element predictions obtained from nonlinear isotropic analyses are in poor agreement with the observed behavior of test sections. Especially, the predicted values of vertical strains on subgrade and radial strains at the bottom of base/AC and the surface deflections in conventional sections are considerably different than the measured values reported for the GA Tech pavement test sections.

Table 21. Comparison of Predicted and Measured Response Variables for Conventional Pavement Sections-- Nonlinear Isotropic

Response	Top Subgrade		Bottom Base		Top Base	Bottom AC		Surface Deflection		
	σ_Z (psi)	ε_Z (10^{-6})	ε_R (10^{-6})	ε_Z (10^{-6})	ε_Z (10^{-6})	ε_R (10^{-6})	ε_Z (10^{-6})	$\delta_{C.L.}$ (in)	$\delta_{10"}$ (in)	$\delta_{14.5"}$ (in)
Section 8	11.9	1850	375	110	560	300	-	-	0.02	0.013
Section 9	11.1	1750	1080	340	560	280	-	-	0.022	0.013
Section 10	6.8	2500	1025	400	620	400	-	-	0.017	0.01
Ave. Measured (Conventional)	9.9	2000	-936	280	580	-330	-	0.028	0.017	0.013
Nonlinear Isotropic										
Texas Model 1st Test	9.7	1222	-437	620	1256	-397	549	0.021	0.011	0.007
Texas Model 2nd Test	10.2	1294	-454	766	1342	-434	587	0.023	0.012	0.008
Texas Model 3rd Test	9.0	1143	-415	449	1053	-328	483	0.018	0.009	0.006
Previous GA Tech Model	8.3	1113	-408	755	736	-324	485	0.019	0.010	0.007
AASHTO T294-94 (6"×12" spec.)	9.8	1236	-451	888	1292	-522	658	0.021	0.010	0.006

Table 22. Comparison of Predicted and Measured Response Variables for Inverted Pavement Sections – Nonlinear Isotropic

Response	Top Subgrade		Bottom Subbase		Bottom Base		Top Base	Bottom AC		Surface Deflection		
	σ_Z (psi)	ε_Z (10^{-6})	ε_R (10^{-6})	ε_Z (10^{-6})	ε_R (10^{-6})	ε_Z (10^{-6})	ε_Z (10^{-6})	ε_R (10^{-6})	ε_Z (10^{-6})	$\delta_{C.L.}$ (in)	$\delta_{10"}$ (in)	$\delta_{14.5"}$ (in)
Measured Responses												
Section 11	3.3	390	-	-	54	370	730	-340	-	0.019	0.007	0.003
Section 12	3.4	340	-	-	22	420	760	-260	-	0.016	0.006	0.003
Nonlinear Isotropic – Section 11												
Texas – 1st Test	4.4	245	-59	35	41	797	1524	-364	532	0.014	0.007	0.004
Texas – 2nd Test	4.5	274	-65	38	49	963	1644	-387	562	0.016	0.008	0.005
Texas – 3rd Test	4.2	226	-56	33	35	599	1276	-309	479	0.012	0.005	0.004
AASHTO T294-94 (12"×6" spec.)	4.1	222	-54	32	37	817	1921	-437	584	0.016	0.007	0.004
Nonlinear Isotropic – Section 12												
Texas – 1st Test	3.6	142	-34	19	28	876	1571	-367	536	0.014	0.006	0.004
Texas – 2nd Test	3.7	157	-37	20	31	1020	1642	-378	555	0.015	0.007	0.005
Texas – 3rd Test	3.6	135	-33	18	26	681	1344	-318	489	0.012	0.005	0.003
AASHTO T294-94 (6"×12" spec.)	3.5	128	-31	17	25	929	2043	-454	599	0.015	0.006	0.004

Test Section Response Predictions from Nonlinear Anisotropic Analyses

Finally, nonlinear anisotropic analyses were performed for the cross-anisotropic, stress sensitive nature of the granular base layer. The AC surfacing and the cement stabilized subbase layers in the inverted sections were again assigned the same linear elastic material properties reported previously in Table 15. The silty sand subgrade was also treated as a nonlinear elastic material and characterized using the bilinear model (see Table 15).

Table 23 summarizes the anisotropic model parameters and the Poisson's ratios used in modeling the granular bases of the GA Tech pavement test sections. The SID scheme was used to compute the five cross-anisotropic properties from the laboratory results conducted at the University of Illinois following the ICAR test protocol. This way, the vertical, horizontal and the shear modulus model parameters were determined. The vertical modulus model parameters for the other models, i.e., previous GA Tech and the AASHTO T294-94, were already known as obtained from the standard modulus test results. The simplified procedure (Tutumluer and Thompson, 1998) summarized next obtained the horizontal and shear modulus model parameters for the previous GA Tech and the AASHTO T294-94 models listed in Table 23 .

Table 23. Anisotropic Model Parameters Used In Modeling Pavement Test Section Response

Nonlinear Anisotropic Analysis										
Anisotropic Runs	Parameters for M_R^{v} †			Parameters for M_R^{h} †			Parameters for G_R †			Poisson's Ratio
	K4 (psi)	K5	K6	K1 (psi)	K2	K3	K7 (psi)	K8	K9	
Previous GA Tech Model	4867	0.80	-0.05	632.7	3.3	-2.45	1459.5	1.0	-0.25	$\nu_v^1 = 0.43$ $\nu_h^1 = 0.15$ $\nu_v^2 = 0.45$ $\nu_h^2 = 0.10$
Texas Model 1st Test	4928.0	0.431	0.171	1168.2	1.088	-0.442	1055.6	0.741	-0.080	$\nu_v = 0.11$ $\nu_h = 0.21$
Texas Model 2nd Test	3090.2	0.496	0.211	1594.8	0.930	-0.374	912.6	0.726	-0.047	$\nu_v = 0.12$ $\nu_h = 0.27$
Texas Model 3rd Test	7446.5	0.417	0.122	1091.1	0.889	-0.186	1078.9	0.754	-0.088	$\nu_v = 0.08$ $\nu_h = 0.18$
AASHTO T294-94 (6"×12" spec.)	6606.7	0.498	-0.079	793	2.998	-2.579	1832.4	0.698	-0.279	$\nu_v^1 = 0.43$ $\nu_h^1 = 0.15$ $\nu_v^2 = 0.45$ $\nu_h^2 = 0.10$

[1] Poisson's ratio for top two sub-layers; [2] Poisson's ratio for bottom sub-layer

† See page 3 of this report

A Simplified Procedure for Determining Anisotropic Model Parameters

To characterize the typical variations of horizontal and shear stiffness ratios, Tutumluer and Thompson (1998) analyzed a conventional flexible pavement section with anisotropic stiffness models used in an 8-in. granular base. The models were obtained from the multiple regression analyses of 50 triaxial test results on different aggregates obtained from the works of Hicks (1970), Allen (1973), and Crockford et al. (1990). The GT-PAVE analyses performed for a variety of aggregate types and properties used in the granular layer typically resulted in horizontal stiffness varying between 5 percent to 30 percent of the vertical, and the shear stiffness between 18 percent to 35 percent of the vertical stiffness under the wheel load throughout the base.

Researchers generally observed that the constant terms in the stiffness ratio models (K_1 /K_4 or K_7 /K_4) were good approximations for the horizontal and shear stiffness ratios (M_R^h/M_R^v and G_R/M_R^v) predicted by the finite element analyses under the wheel load. Figure 11 shows the variations of the constant terms in the shear (K_7 /K_4) and horizontal (K_1 /K_4) stiffness ratio models obtained from tests performed on a variety of crushed (C) and partially crushed (PC) aggregates and gravel (see Introduction section of this report). Although somewhat scattered, the data points plotted at various saturation levels clearly indicate an increasing trend of K_7 /K_4 (thus G_R/M_R^v) with K_1 /K_4 (thus M_R^h/M_R^v). The dotted lines plotted around the data define the lower and upper bounds for a typical variation of K_7 /K_4 with K_1 /K_4 from triaxial test results for which the horizontal and shear stiffness proportionally increase or decrease. Accordingly, a granular material with high shear and horizontal stiffness would have a reduced tendency to lateral spreading under wheel loads. Figure 11 also presents an excellent linear relationship found to exist between the constant shear ratio K_7 /K_4 and the constant horizontal ratio K_1 /K_4 for a very consistent set of 9 test results reported by Allen (1973). The standard estimated error (SEE) in the equation (see Figure 11) was given as 0.00636 for K_7 /K_4.

Based on the data presented by Hicks (1970), Allen (1973), and Crockford et al. (1990), Tutumluer and Thompson (1998) established a procedure for estimating cross-anisotropic properties from repeated load triaxial tests in which only vertical deformations were measured (the standard procedure, i.e., AASHTO T 294-94). To estimate horizontal and shear model

parameters, an additional equation was also given relating the shear model constant parameter K_7 with the vertical model parameters K_4, K_5, and K_6 as follows:

$$K_7 \text{ (psi)} = -90.92 + 0.27\ K_4 + 305.34\ K_5 + 158.22\ K_6 \quad (R^2 = 0.94, SEE = 178 \text{ psi}) \qquad (4)$$

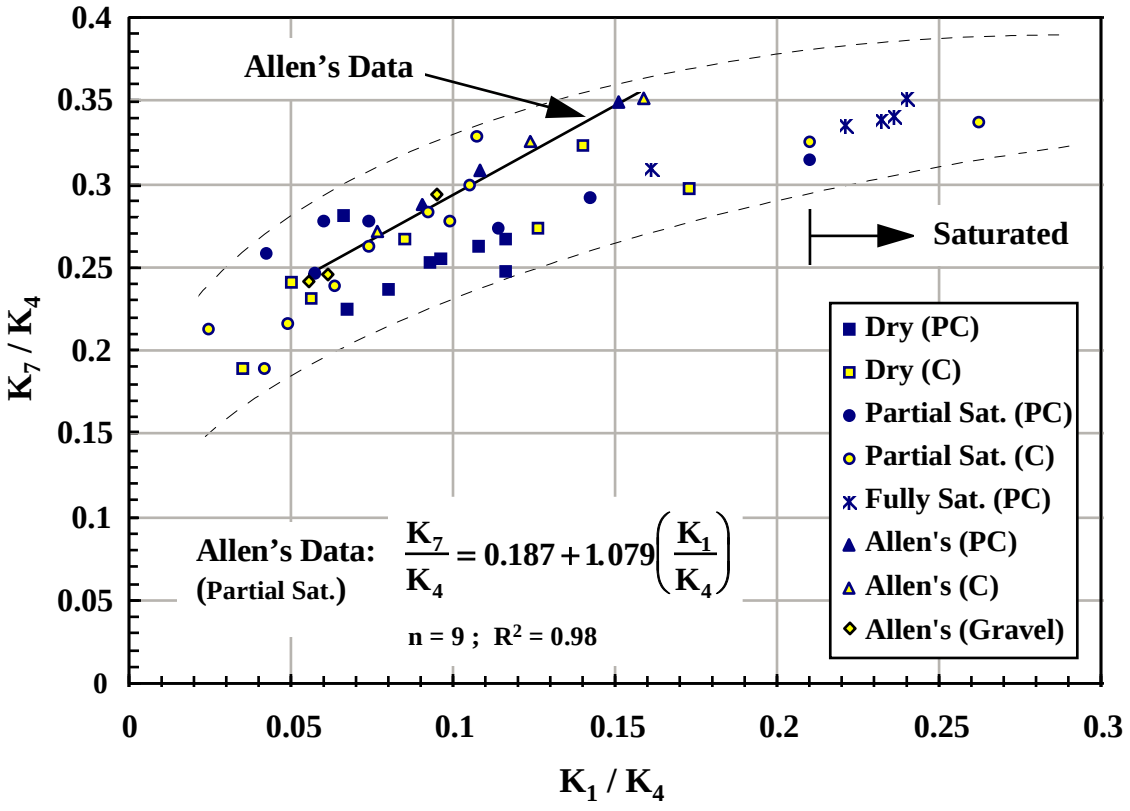

Figure 11. Variation of Constant Ratios in Horizontal and Shear Stiffness Ratio Models (after Tutumluer and Thompson, 1998)

Figures 12 and 13 show for the 50 test results the deviator stress exponents (K_3-K_6 or K_9-K_6) plotted with the bulk stress exponents (K_2-K_5 or K_8-K_5) as obtained from the horizontal and shear stiffness ratio models. In both plots, the data points are generally centered on the equality line indicating that they are equal in magnitude but opposite in sign. Overall, these plots indicate that when deviator and bulk stresses take similar values under the applied wheel load, the constant ratio terms in the models play the governing role in determining the stiffness ratios.

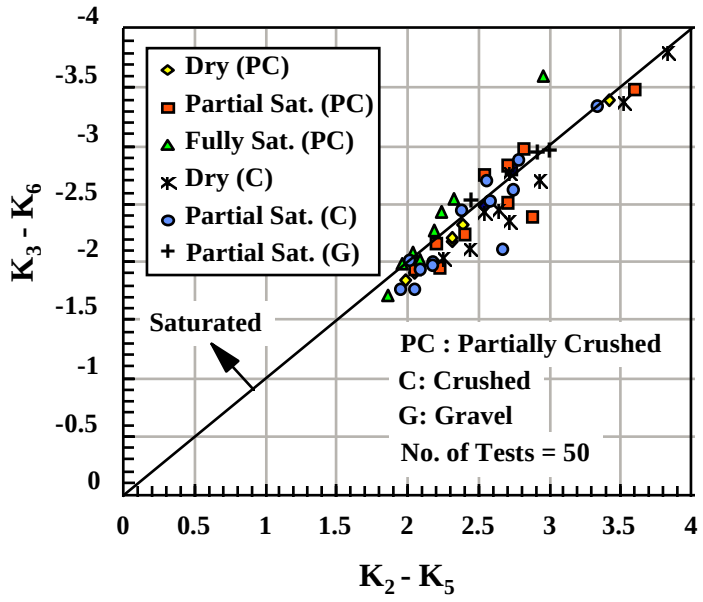

Figure 12. Variation of Stress Exponents in the Horizontal Stiffness Ratio Model (after Tutumluer and Thompson, 1998)

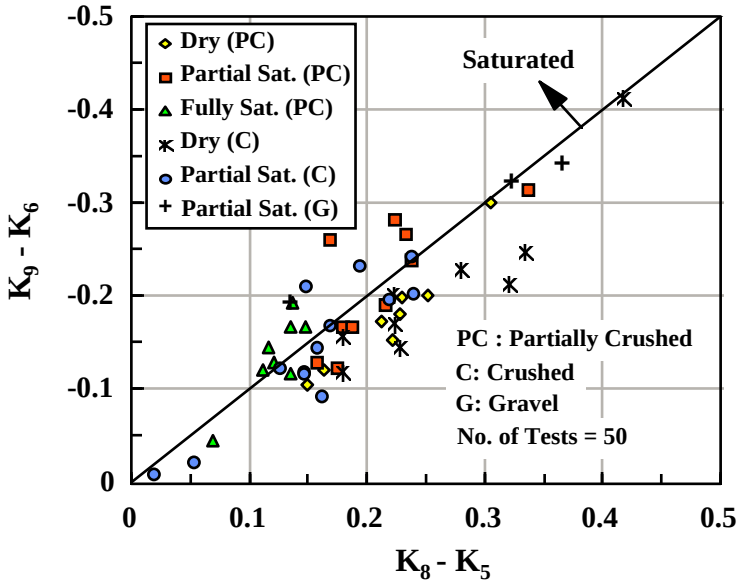

Figure 13. Variation of Stress Exponents in the Shear Stiffness Ratio Model (after Tutumluer and Thompson, 1998)

According to the above outlined simplified procedure by Tutumluer and Thompson (1998), the following steps were followed to estimate the shear and horizontal model parameters for the previous Georgia Tech and the AASHTO T294-94 models listed in Table 23, knowing the experimentally determined vertical modulus models:

(1) use Equation 4 to compute K_7;

(2) compute the constant ratio K_7 / K_4;

(3) use the upper and lower band as well as Allen's linear fit indicated in Figure 11 to obtain the corresponding K_1/K_4 constant ratio;

(4) from Figure 12, select values - equal in magnitude but opposite in sign - for the stress exponents K_2-K_5 and K_3-K_6 to be used in the horizontal stiffness ratio model (an approximate value of 2.5 has been used as suggested by Tutumluer and Thompson, 1998); and finally,

(5) from Figure 13, select values - equal in magnitude but opposite in sign - for the stress exponents K_8-K_5 and K_9-K_6 to be used in the shear stiffness ratio model (an approximate value of 0.2 has been used as suggested by Tutumluer and Thompson, 1998). Note that due to the very low to nonexistent horizontal compressive confining pressures under the wheel load, approximating these stress exponents does not have any significant effect in the overall anisotropic dilative behavior of granular bases.

Tables 24 and 25 compare the measured response variables with GT-PAVE predictions for the conventional and inverted sections, respectively. Former response predictions by Tutumluer (1995) are also listed for comparison. In general, the anisotropic GT-PAVE FE predictions are in reasonably good agreement with the observed behavior of both the conventional and inverted sections. Although the previous Georgia Tech model did not converge to provide nonlinear solutions for inverted sections, it gave the best results for the conventional sections with predictions closely matching both the former predictions obtained by Tutumluer (1995) and the measured responses. This is mainly due to the fact that the analysis used the same vertical modulus model, which was obtained from previous test results on the original granitic gneiss placed in the test sections nearly 20 years ago.

Table 24. Comparison of Predicted and Measured Response Variables for Conventional Pavement Sections – Nonlinear Anisotropic

Response	Top Subgrade		Bottom Base		Top Base	Bottom AC		Surface Deflection		
	σ_Z (psi)	ε_Z (10^{-6})	ε_R (10^{-6})	ε_Z (10^{-6})	ε_Z (10^{-6})	ε_R (10^{-6})	ε_Z (10^{-6})	$\delta_{C.L.}$ (in)	$\delta_{10"}$ (in)	$\delta_{14.5"}$ (in)
Section 8	11.9	1850	375	110	560	300	-	-	0.02	0.013
Section 9	11.1	1750	1080	340	560	280	-	-	0.022	0.013
Section 10	6.8	2500	1025	400	620	400	-	-	0.017	0.01
Ave. Measured (Conventional)	9.9	2000	-936	280	580	-330	-	0.028	0.017	0.013
Nonlinear Anisotropic										
Former Predictions by Tutumluer (1995)	9.5	2080	-985	478	626	-384	553	0.026	0.017	0.013
Texas Model 1st Test	12.1	1664	-627	621	1140	-535	688	0.025	0.013	0.009
Texas Model 2nd Test	12.5	1613	-565	801	1282	-562	712	0.026	0.014	0.009
Texas Model 3rd Test	12.2	1678	-627	469	945	-509	664	0.024	0.012	0.008
Previous GA Tech Model	10.9	1991	-955	492	632	-415	591	0.024	0.012	0.008
AASHTO T294-94 (6"×12" specimen)	11.4	2023	-951	695	1300	-611	751	0.026	0.013	0.009

Table 25. Comparison of Predicted and Measured Response Variables for Inverted Pavement Sections – Nonlinear Anisotropic

Response	Top Subgrade		Bottom Subbase		Bottom Base		Top Base	Bottom AC		Surface Deflection		
	σ_Z (psi)	ε_Z (10^{-6})	ε_R (10^{-6})	ε_Z (10^{-6})	ε_R (10^{-6})	ε_Z (10^{-6})	ε_Z (10^{-6})	ε_R (10^{-6})	ε_Z (10^{-6})	$\delta_{C.L.}$ (in)	$\delta_{10"}$ (in)	$\delta_{14.5"}$ (in)
Measured Responses												
Section 11	3.3	390	-	-	54	370	730	-340	-	0.019	0.007	0.003
Section 12	3.4	340	-	-	22	420	760	-260	-	0.016	0.006	0.003
Nonlinear Anisotropic – Section 11												
Former Predictions by Tutumluer (1995)	4.0	390	-79	45	51	317	1050	-348	536	0.016	0.009	0.006
Texas – 1st Test	4.8	339	-81	46	68	976	1476	-442	616	0.016	0.007	0.005
Texas – 2nd Test	4.9	340	-82	46	71	1167	1627	-463	639	0.018	0.009	0.006
Texas – 3rd Test	4.9	358	-85	48	72	791	1240	-406	585	0.014	0.007	0.004
AASHTO T294-94 (12"×6" specimen)	4.7	238	-61	37	42	546	1740	-544	687	0.017	0.007	0.004
Nonlinear Anisotropic – Section 12												
Former Predictions by Tutumluer (1995)	3.5	236	-46	25	35	362	1047	-341	532	0.015	0.008	0.006
Texas – 1st Test	3.9	183	-44	23	39	1060	1528	-438	612	0.015	0.007	0.004
Texas – 2nd Test	4.1	178	-43	23	39	1330	1779	-479	651	0.017	0.008	0.005
Texas – 3rd Test	4.0	192	-46	24	42	872	1297	-402	582	0.013	0.006	0.004
AASHTO T294-94 (6"×12" specimen)	3.7	155	-37	20	29	481	1752	524	-673	0.016	0.006	0.004

The new cross-anisotropic models developed in this validation study are the Texas models, and the AASHTO T294-94 model listed in Tables 24 and 25. The Texas models used data from tests I, II, and III conducted following the ICAR test protocol, whereas the AASHTO T294-94 model was developed from the results of a standard modulus test performed on a 6 in. diameter by 12 in. high specimen. All Texas models produced very consistent response predictions. The lowest vertical strains, also the closest ones to the measured responses, were predicted in the granular base by the Texas-3 model obtained from Test III with only 4 percent fines allowed in the aggregate gradation. This is in accordance with the highest vertical percent moduli obtained for Test III material from laboratory results (see Figures 8 and 9). Considering the fact that the anisotropic properties of the Norcross crushed stone was evaluated approximately 20 years after the original pavement sections were constructed and tested, the SID scheme and the ICAR protocol produced quite adequate characterization models from the laboratory data. The predicted values of both surface deflections and vertical strain/stress on the subgrade compare well with the order of magnitudes of the measured responses in the conventional and inverted sections.

The AASHTO T294-94 model predictions are also in good agreement with the observed behavior of the test sections. In essence, the simplified procedure (Tutumluer and Thompson, 1998) followed to establish anisotropic models from the standard modulus test results worked quite well. The predicted values of surface deflections, vertical strain/stress on the subgrade, and radial strain at the bottom of base match somewhat closely the measured responses in the conventional and inverted sections. Yet the vertical strains predicted at top and bottom of base in both conventional and inverted sections are typically greater than the measured values. This indicates that the granitic gneiss used in the pavement test sections was actually much stronger under similar stress states.

The vertical modulus distribution within the nonlinear unstabilized aggregate base is graphed in Figure 14 as predicted by the Texas-3 model. The modulus values were obtained at the middle of elements and plotted as equal contour lines in the granular base of the conventional sections. Models predicted maximum modulus of 49 ksi at the top of the base. The moduli are typically decreasing with increasing granular base depth and radial offset distance, which

properly capture a nonlinear stress dependent type UAB stiffness response. In Figure 15, the anisotropic modular ratios (M_R^h/M_R^v) obtained from the Texas-3 model are also plotted within the base layer. Note that the ratios only get a high of 0.27 at the top of the base and then decrease to 0.17 with the increasing depth and radial offset distance. Such a variation is in accordance with the range of typical ratios reported by Tutumluer and Thompson, (1998).

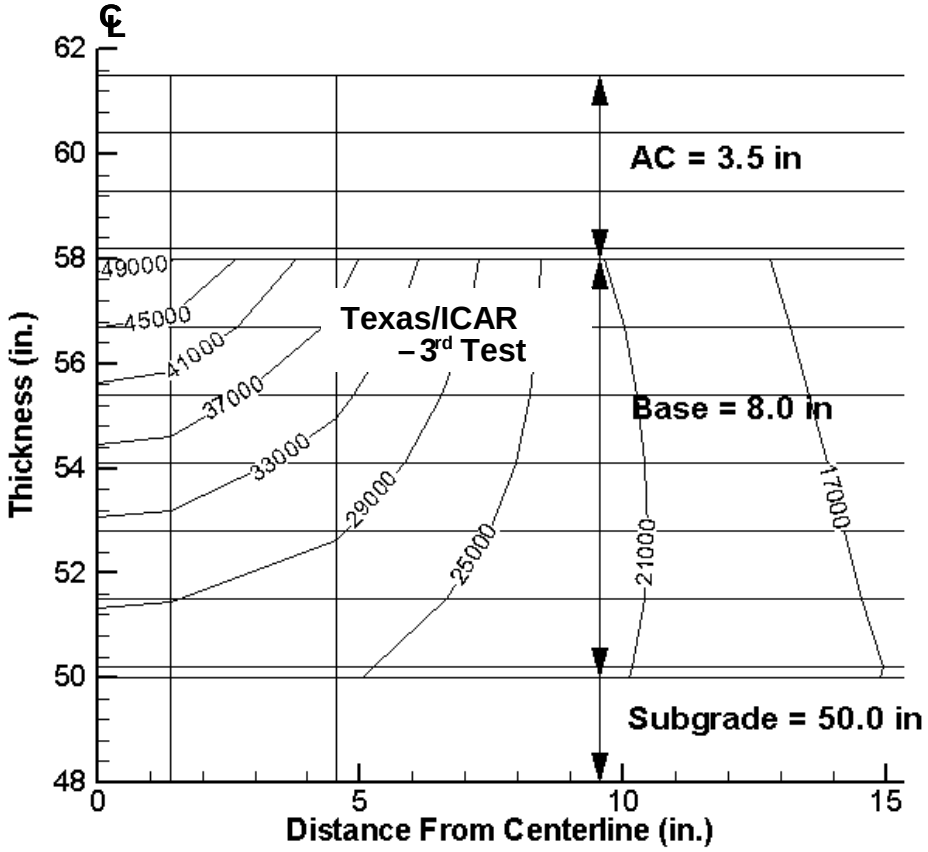

Figure 14. Vertical Modulus Distribution within the Base Predicted by Texas-3 Model

Figure 16 shows the vertical modulus distribution within the nonlinear unstabilized aggregate base predicted by the AASHTO T294-94 model. The modulus values were obtained at the middle of elements and plotted as equal contour lines in the granular base of the conventional sections. A maximum modulus of only 28 ksi was computed at the top of the base when compared to the 49 ksi predicted at the same location by the Texas-3 model. Note that such low moduli assigned in the granular layer are in accordance with the low moduli

determined from the standard modulus test results (see Figure 9) and explain why higher vertical strains were predicted at top and bottom of base in both conventional and inverted sections when compared to the measured values. Furthermore, the anisotropic modular ratios (M_R^h/M_R^v) computed from the AASHTO T294-94 model were found to be almost a constant 0.12 throughout the base layer, which is in compliance with the K_1/K_4 ratio established from the simplified procedure.

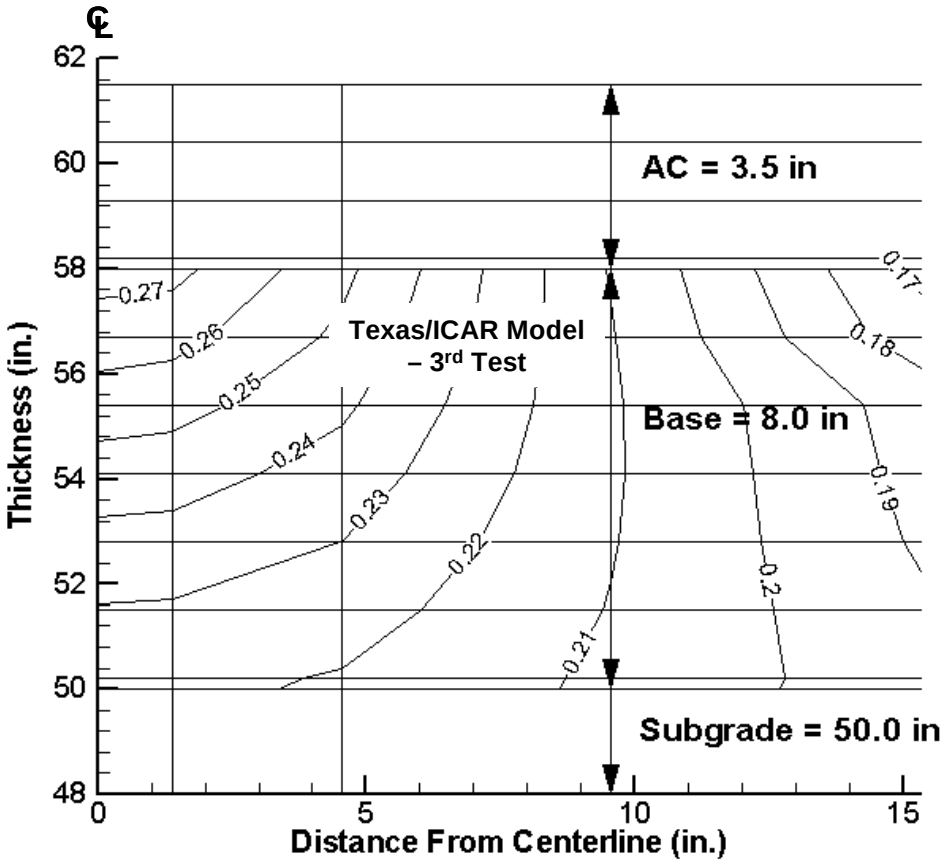

Figure 15. Modular Ratio (M_R^h/M_R^v) Distribution within the Base Predicted by Texas-3 Model

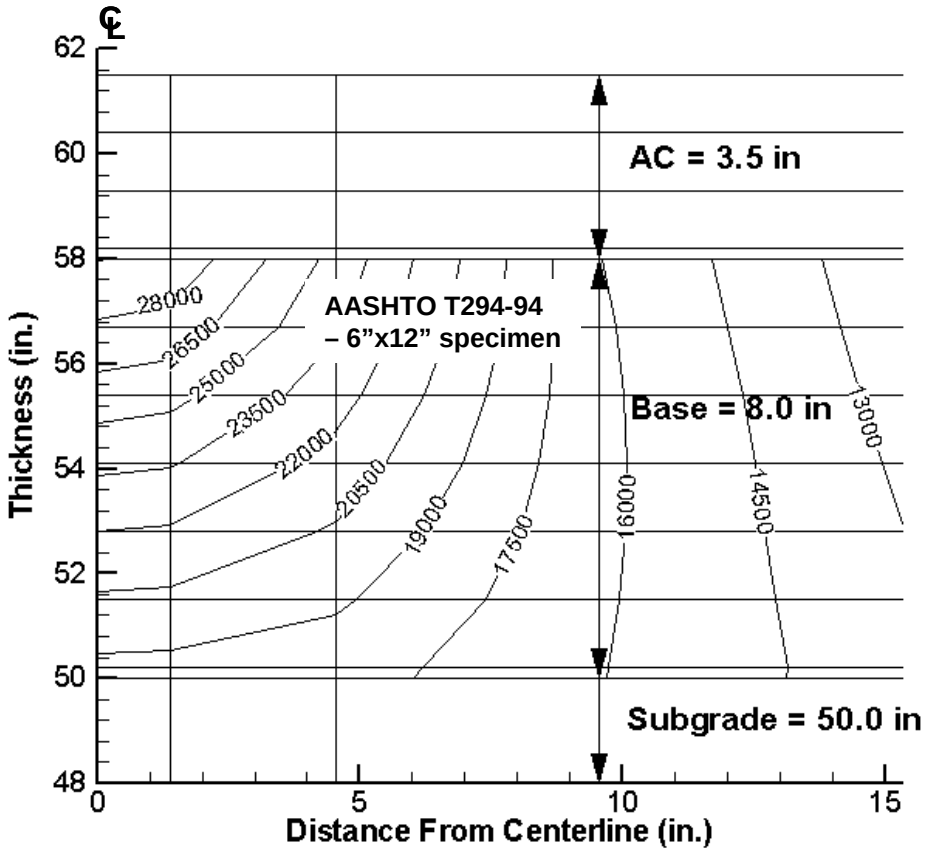

Figure 16. Vertical Modulus Distribution within the Base Predicted by AASHTO T294-94 Model

Stress States from Anisotropic Modeling

Previous studies and ICAR Project 502 reports indicated that anisotropic modeling achieves a more realistic stress distribution in UABs than that developed when the aggregate base is considered to be linear and isotropic (Tutumluer, 1998 and Adu-Osei et al., 2000). The stress distribution based on cross-anisotropic analysis is not only more correct, but it is also more favorable to the unbound aggregate in that significant tensile stresses do not occur. An aggregate base cannot accommodate such tensile stresses and therefore a compensating adjustment is required. The analogy given was that the response of the aggregate base to the load is as if the stress distribution directly under the wheel load due to anisotropy acts as a moving column under the wheel in which the aggregate essentially produces its own confinement and does not enter into tension.

Figure 17 compares centerline radial stresses predicted from different analyses in the conventional section. Linear elastic analysis results are presented for the 60-ksi constant modulus case only. In addition, radial stresses predicted from both the isotropic and anisotropic versions of the nonlinear models, Texas-3, Previous GA-Tech, and the AASHTO T294-94, are shown.

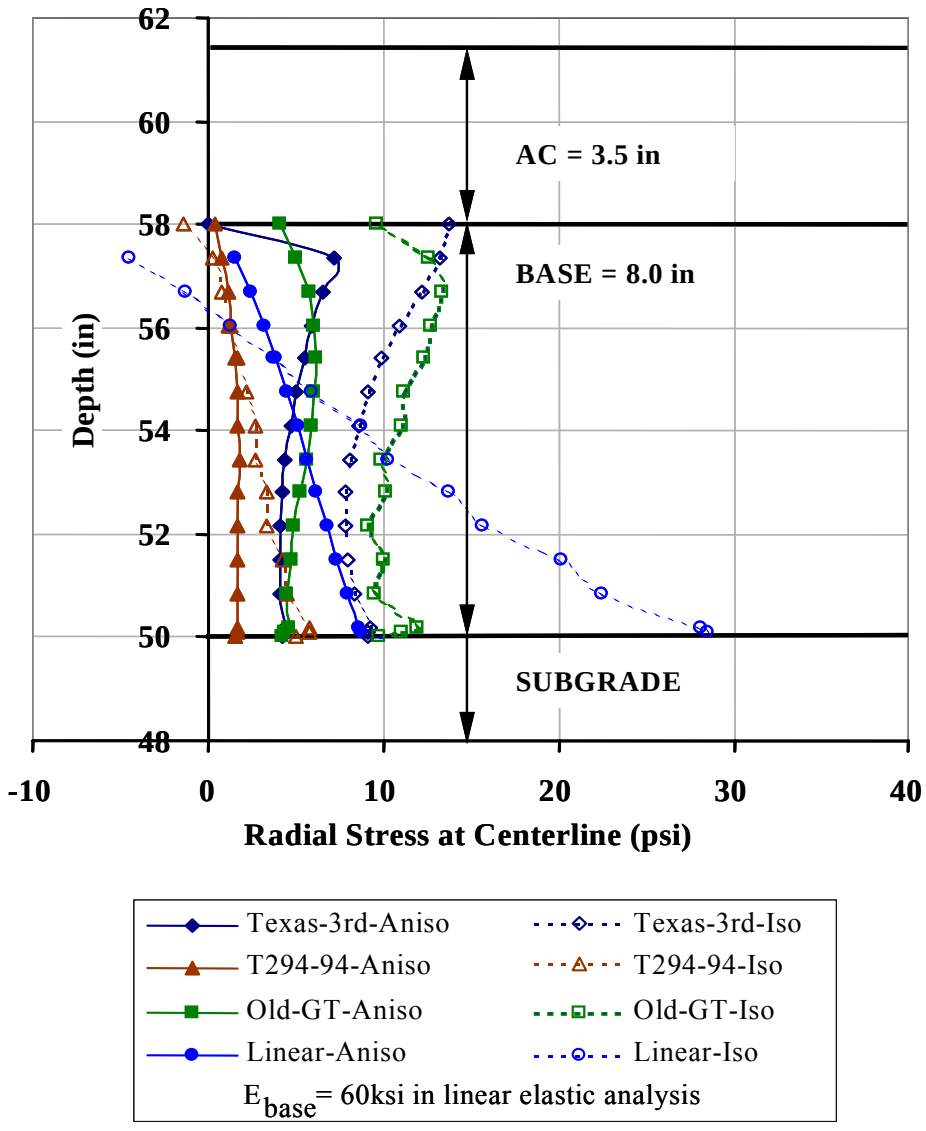

Figure 17. Distribution of Centerline Radial Stresses within the Base Predicted by Different Analyses

The computed radial tensile stresses gradually decrease with increased sophistication in material characterization and improved structural modeling (see Figure 17). Going from a linear

elastic analysis to a nonlinear, stress sensitive UAB characterization, the predicted tensile stresses often decrease by some amount. Nonetheless, nonlinear isotropic analyses alone do not generally result in tensile stresses low enough to be considered admissible in the granular layer. Drastic reductions in the predicted horizontal tension are achieved when using nonlinear cross-anisotropy as compared to a linear isotropic analysis. For example, an unjustifiably high 28-psi radial tensile stress predicted at the bottom of base by the linear isotropic analysis decreases to less than a 5-psi value from nonlinear anisotropic analyses (see Figure 17). Such low tensile stresses predicted by the continuum modeling of the UAB layer could be at least partly explained by the shear resistance of unbound aggregates under vertical compressive stresses using a particulate mechanics modeling approach as recently taken by Tutumluer and Barksdale (1998).

The total elimination of tensile stresses could also be achieved by employing the nonlinear anisotropy in the granular base and considering the offsetting effects of the compaction induced residual stresses. In the past, inclusion of a constant 3-psi compressive residual stress in the nonlinear analysis was found to eliminate tensile stresses (Tutumluer, 1998). In that case, the unbound aggregate base was completely in compression, with radial compressive stresses increasing away from the centerline.

For the inverted sections, analysis determined the unbound aggregate base to be completely in compression with radial compressive stresses increasing away from the centerline. As a result of placing the cement-stabilized layer beneath the unstabilized crushed stone base, primarily horizontal compressive stresses are developed in the base. An important factor in achieving good performance of an inverted section is to provide a stabilized subbase having sufficient strength to prevent fatigue and durability related failures.

SUMMARY AND CONCLUSIONS

The efforts in this ICAR 502 project validation study have been primarily aimed at demonstrating the actual anisotropic and stress dependent behavior of unbound aggregate bases used in flexible pavements. Previous laboratory work has indicated that with anisotropic modeling a more realistic stress distribution can be achieved in the UABs than that developed when the aggregate base is considered to be linear and isotropic. With stress states more correctly predicted in the UABs, a better characterization of the excellent compressive characteristics of the high quality aggregates is also achieved. This will help promote the increased use of unbound aggregate layers as major structural components in flexible pavements.

Field validation data were collected from two previous full-scale pavement test studies, Texas Transportation Institute and Georgia Tech studies. Researchers validated the nonlinear anisotropic behavior of UBAs by analyzing these full-scale pavement test sections using TTI-PAVE and GT-PAVE finite element (FE) programs, predicting UAB responses, and comparing them to the measured ones.

TTI PAVEMENT TEST SECTIONS

The TTI project dealt with two flexible pavement test sections, having both a thin asphalt surface and a thick asphalt surface layer, built at the TTI Research Annex. The base course in each pavement was a crushed Texas limestone meeting TXDOT Grade 1, Item 248, aggregate base specifications. The test sections were instrumented with multi-depth deflectometers. A falling weight deflectometer was positioned directly over the MDD and at several different positions away from MDD and pavement response (deflections) was collected. FWD data were used to backcalculate material properties of the two pavement sections. For validation of the anisotropic resilient behavior, the limestone was characterized in the laboratory according to the ICAR testing protocol.

Based on the FWD surface deflections and MDD depth deflections, several computer runs were made using the TTI-PAVE FE program with different material properties until the

average percent error in deflections was less than 10 percent. In the TTI-PAVE runs, the surface layer and subgrade were assumed to be linearly elastic and the base layer was assumed to be nonlinear cross-anisotropic. The base layer was then analyzed as linear isotropic, nonlinear isotropic, and linear cross-anisotropic and the deflections computed were compared to the measured deflections. Much higher percent errors between the measured and predicted deflections were obtained from the linear elastic analyses when compared to those obtained from the nonlinear isotropic and cross-anisotropic analyses. The nonlinear cross-anisotropic material models used in the base layer predicted vertical deflections that are close to field deflections in the analyzed TTI pavements.

GA TECH PAVEMENT TEST SECTIONS

The second full-scale pavement test study considered, which had extensive instrumentation done and the responses measured in the UABs, was conducted by Barksdale, and Todres, (1983) in A Study of Factors Affecting Crushed Stone Base Performance, Final Report, Georgia Institute of Technology Report SCEGIT-82-109, Atlanta, GA. The pavements studied with granular bases consisted of three conventional sections and two inverted sections, which had an unbound aggregate base sandwiched between an upper asphalt concrete surfacing and a lower cement stabilized subbase. A total of eight response parameters, stresses, and strains at different locations in the test sections together with surface deflections, were measured from each test performed, using primarily strain gages, Bison type pressure cells, and LVDTs.

The aggregate material used in the granular base layers of the GA Tech pavement test sections was a granitic gneiss, referred to as the Norcross crushed stone, which was obtained for this validation study from the Norcross Quarry of Vulcan Materials Co. Special attention was given to properly re-engineer the Norcross crushed stone such that its size properties, i.e., gradation and fines content, would be comparable to those reported for the original granitic gneiss used in the GA Tech test sections. Nonetheless, other properties affecting laboratory evaluation of the aggregate for modulus and deformation characteristics such as the shape properties (flatness and elongation, angularity, surface texture, etc.) and achieved compaction properties could not be verified and therefore might not have been the same with the granitic

gneiss constructed and tested nearly 20 years ago. Laboratory testing of the aggregate samples was conducted at the University of Illinois and characterization models were developed for the stress sensitive, cross-anisotropic aggregate behavior.

Researchers next predicted the resilient responses of the conventional and inverted pavement test sections using the GT-PAVE FE program at different locations in the test sections considering several methods of UAB characterization for comparison and field validation. These included:

(1) a linear elastic, isotropic analysis,
(2) a linear elastic, cross-anisotropic analysis,
(3) a nonlinear, stress sensitive isotropic analysis,
(4) characterization of the vertical resilient modulus as nonlinear stress sensitive according to a Uzan type model and then assuming that the horizontal modulus is some percentage of the vertical modulus (work done by Tutumluer, 1995),
(5) a nonlinear stress sensitive cross-anisotropic analysis using modulus models developed following the laboratory SID approach (Adu Osei et al., 2000), and
(6) a nonlinear stress sensitive cross-anisotropic analysis with model parameters obtained from a simplified procedure that uses AASHTO T294-94 resilient modulus test results and adopted earlier by Tutumluer and Thompson (1998).

The modeling results obtained from the different analyses employed, i.e., linear elastic layered with isotropic and anisotropic base, nonlinear isotropic, and nonlinear anisotropic layered analysis, were compared for prediction performance. In contradiction with the linear isotropic analysis results (method 1), the finite element predictions obtained from the linear anisotropic analyses (method 2) were in reasonably good agreement with the observed behavior of test sections. Furthermore, the finite element predictions obtained from nonlinear isotropic analyses (method 3) were not in good agreement with the observed behavior of test sections. Especially, the predicted values of vertical strains on subgrade and radial strains at the bottom of base/AC and the surface deflections in conventional sections were considerably different than the measured values reported for the GA Tech pavement test sections. Such a finding is actually in

accordance with the previous observation reported by Barksdale et al. (1989) in that a linear anisotropic analysis of an UAB could give better predictions than a nonlinear isotropic analysis.

The accuracy of the overall modeling of resilient behavior of both the conventional and inverted sections was related to how well the measured response variables were predicted at the same time. Only when using in the UAB a *nonlinear cross-anisotropic model* developed by Tutumluer (either method 4 or method 6), the resilient behavior of five pavement test sections were predicted *at the same time* reasonably accurately for up to 8 response variables (i.e., displacements, stresses and strains). Such predictions are hard to achieve and indicate that the GT-PAVE FE model used is reasonably valid and the original characterization model, GA Tech model, developed for the Norcross crushed stone still characterized best the stress sensitive, cross-anisotropic aggregate behavior.

The new cross-anisotropic models developed in this validation study were the Texas/ICAR models, and the AASHTO T294-94 model. The Texas/ICAR models used data from tests conducted following the ICAR test protocol, whereas the AASHTO T294-94 model was developed from the results of a standard modulus test performed on a 6 in. diameter by 12 in. high specimen. All Texas/ICAR models produced very consistent and reasonably good response predictions. Considering the fact that the anisotropic properties of the Norcross crushed stone was evaluated nearly 20 years after the original pavement sections were constructed and tested, the SID scheme and the ICAR protocol produced quite adequate characterization models from the laboratory data. The AASHTO T294-94 model predictions were also in good agreement with the observed behavior of the test sections. In essence, the simplified procedure (Tutumluer and Thompson, 1998) followed to establish anisotropic models from the standard modulus test results worked quite well.

A stress sensitive, cross-anisotropic representation of the base was shown to greatly reduce the horizontal tension predicted in the granular base when compared to a linear isotropic representation. The radial tensile stresses computed at the centerline of conventional sections gradually decreased with increased sophistication in material characterization and improved structural modeling. Use of a small percentage, typically in the range of 12 percent to 27

percent, of the vertical modulus in the horizontal direction was necessary for: (1) predicting correctly the horizontal and vertical measured strains in the base layers, and (2) properly modeling the horizontal tension in the granular base layer.

RESEARCH NEEDS FOR IMPLEMENTATION

The ICAR laboratory work to date has evaluated only a limited number of aggregate types and sources for determining anisotropic properties since advanced triaxial testing equipment is required to perform these tests in the laboratory. The University of Illinois FastCell and the IPC Cell used by TTI are the only equipment that can be utilized in the laboratory. Testing of more aggregate types and sources is needed. By testing a broader suite of materials, important parameters contributing to anisotropic aggregate behavior such as gradation, particle shape, particle texture, etc. will be identified.

This project indicates a need for a database containing anisotropic properties and characterization model parameters for the broader suite of materials obtained from aggregate producers throughout the country. Once such a database is formed, it will be possible to relate anisotropic model parameters to the resilient moduli obtained from the standard AASHTO test procedure (AASHTO T 294-94; "Resilient Modulus Testing of Unbound Granular Base/Subbase Materials and Subgrade Soils" - SHRP Protocol P46), which does not provide for radial specimen deformation measurements. A simplified procedure, similar to the one proposed by Tutumluer and Thompson (1998) and used in this validation report, should be established to obtain anisotropic characterization model parameters and recommended for use to the NCHRP research team working on the development of the 2002 Guide or the future versions of this Guide.

It is necessary to assess an immediate approach to UAB characterization that is as simple to use as possible without compromising the ability to adequately characterize the UAB. This can be an interim, quick to implement linear anisotropic approach or the full nonlinear characterization developed from the database concept presented earlier. Whichever approach is taken, a set of recommendations/guidelines for the selection of percent reductions in the vertical modulus to be assigned for the horizontal and shear moduli has to be still developed based on experimental results. This kind of an approach will be the method with the most utility to the aggregates industry for pavement design and analysis at this time.

A large stress excursion analysis will be needed to further validate and refine the model to characterize UAB behavior under various stress path loadings. This step requires more elaborate testing to be conducted on laboratory specimens for modeling response to rolling wheels, which involves rotation of principal planes and inelastic and dynamic interpretations of the data. This is a more comprehensive effort since the aggregate rutting potentials under different stress paths will also have to be studied. Note that stress path loadings different than the one applied in the standard constant confining triaxial tests (AASHTO T294-94) have been shown in previous studies to increase accumulated permanent strains. In essence, for controlling rutting in the field, UAB behavior due to rolling wheels has to be studied.

More instrumented pavement sections need to be built to obtain a large field database for further validation of the finite element program. Existing modulus backcalculation methods use linear layered elastic techniques. It is extremely difficult to use finite element methods to backcalculate layer material properties. Findings point to further research incorporating anisotropy and material nonlinearity in backcalculation methods to account for the behavior of unbound granular layers.

Finally, the aggregates industry must be proactive in providing funding to support these immediate research needs. It is also essential to recommend the use of the superior anisotropic aggregate characterization and performance models in order to have these models available for use and incorporation into the design guides. The industry must make this information available to the NCHRP research team during the development of the 2002 Guide and its future versions to ensure that the Guide will accurately and equitably incorporate aggregate pavement layers into the pavement structure.

REFERENCES

AASHTO T294-94 (1995), Resilient Modulus of Unbound Granular Base/Subbase Materials and Subgrade Soils – SHRP Protocol P46. Standard Specifications for Transportation Materials and Methods of Sampling and Testing, Seventeenth Edition, American Association of State Highway and Transportation Officials, Washington D.C.

Adu-Osei, A., D.N Little, and R.L. Lytton, (2000), Structural Characteristics of Unbound Aggregate Bases to Meet AASHTO 2002 Design Requirements. Interim Report, International Center for Aggregate Research (ICAR) Project 502, Texas Transportation Institute, Texas A&M University, College Station, TX, July.

Allen, J.J. (1973), The Effects of Non-constant Lateral Pressures on the Resilient Response of Granular Materials. Ph.D. Dissertation, Department of Civil Engineering, University of Illinois, Urbana, IL, May.

Barksdale, R.D., and H.A. Todres (1983), A Study of Factors Affecting Crushed Stone Base Performance. Final Report, Georgia Institute of Technology Report SCEGIT-82-109, Atlanta, GA.

Barksdale, R.D., S.F. Brown, and F. Chan, (1989), *Potential Benefits of Geosynthetics In Flexible Pavements*. NCHRP Report 315, Transportation Research Council, Washington D.C.

Crockford, W.W., L.J. Bendana, W.S Yang, S.K. Rhee, and S.P. Senadheera, (1990), Modeling Stress and Strain States in Pavement Structures Incorporating Thick Granular Layers. Final Report, Contract F08635-87-C-0039, The Texas Transportation Institute, The Texas A&M University, College Station, Texas, April.

Hicks, R.G. (1970), Factors Influencing the Resilient Properties of Granular Materials. Ph.D. Dissertation, Institute of Transportation and Traffic Engineering, University of California, Berkeley, May.

Hicks, R.G. and C.L. Monismith (1971), Factors Influencing the Resilient Properties of Granular Materials. In Transportation Research Record 345, TRB, National Research Council, Washington D.C., pp. 15-31.

Pezo, R.F. (1993), A General Method of Reporting Resilient Modulus Tests of Soils - A Pavement Engineer's Point of View. Paper No: 93082, Transportation Research Board, 72nd Annual Meeting, National Research Council, Washington, D.C.

Scullion, T., Uzan, J., J.I Yazdani, and P. Chan (1988), Field Evaluation of the Multi-Depth Deflectometers. Texas Transportation Institute Research Report 1123-2, College Station, TX.

Thompson, M.R. and R.P. Elliot (1985), ILLI-PAVE Based Response Algorithms for Design of Conventional Flexible Pavements. In Transportation Research Record 1043, TRB, National Research Council, Washington D.C., pp. 50-57.

Tutumluer, E. (1995), *Predicting Behavior of Flexible Pavements with Granular Bases*. Ph.D. Dissertation, School of Civil and Environmental Engineering, Georgia Institute of Technology, Atlanta, GA, September.

Tutumluer, E. and R.D. Barksdale (1995), Behavior of Pavements with Granular Bases - Prediction and Performance. In Proceedings of the UNBAR4 Symposium, July 17-19, Nottingham, UK, Edited by Dawson A.R. and Jones R.H., pp. 173-183.

Tutumluer, E. and M.R. Thompson (1997a), Anisotropic Modeling of Granular Bases in Flexible Pavements. In *Transportation Research Record 1577*, TRB, National Research Council, Washington D.C., pp. 18-26.

Tutumluer, E. and M.R. Thompson (1997b), Granular Base Moduli for Mechanistic Pavement Design. Proceedings of the ASCE *Airfield Pavement Conference*, Seattle, Washington, August 17-20, pp. 33-47.

Tutumluer, E. and R.D. Barksdale (1998), Analysis of Granular Bases Using Discrete Deformable Blocks. Journal of Transportation Engineering, ASCE, Vol. 124, No. 6, November/December, pp. 573-581.

Tutumluer, E. (1998), Anisotropic Behavior of Unbound Aggregate Bases - State of the Art Summary. Proceedings of the *6th Annual Symposium of the International Center for Aggregate Research (ICAR)*, St. Louis, Missouri, April 19-21, pp. 11-33.

Tutumluer, E. and M.R. Thompson (1998), Anisotropic Modeling of Granular Bases. Final Report to Federal Aviation Administration Center of Excellence for Airport Pavements, COE Report No. 2, Civil Engineering, University of Illinois at Urbana-Champaign.

Uzan, J. (1985), Characterization of Granular Materials. In Transportation Research Record 1022, TRB, National Research Council, Washington D.C., pp. 52-59.

Uzan, J. and T. Scullion (1990), Verification of Backcalculation Procedures. Third International Conference on Bearing Capacity of Roads and Airfields, Trondheim, Norway, pp. 447-458.